



HAL
open science

Influence of low-frequency variability on groundwater level trends

Lisa Baulon, Delphine Allier, Nicolas Massei, H el ene Bessiere, Matthieu Fournier, Violaine Bault

► **To cite this version:**

Lisa Baulon, Delphine Allier, Nicolas Massei, H el ene Bessiere, Matthieu Fournier, et al.. Influence of low-frequency variability on groundwater level trends. *Journal of Hydrology*, 2022, 606, pp.127436. 10.1016/j.jhydrol.2022.127436 . hal-03558802

HAL Id: hal-03558802

<https://hal.science/hal-03558802v1>

Submitted on 22 Jul 2024

HAL is a multi-disciplinary open access archive for the deposit and dissemination of scientific research documents, whether they are published or not. The documents may come from teaching and research institutions in France or abroad, or from public or private research centers.

L'archive ouverte pluridisciplinaire **HAL**, est destin ee au d ep ot et  a la diffusion de documents scientifiques de niveau recherche, publi es ou non,  emanant des  tablissements d'enseignement et de recherche fran ais ou  trangers, des laboratoires publics ou priv es.



Distributed under a Creative Commons Attribution - NonCommercial 4.0 International License

Influence of low-frequency variability on groundwater level trends

Lisa Baulon^{a,b*}, Delphine Allier^b, Nicolas Massei^a, H el ene Bessiere^b, Matthieu Fournier^a, Violaine Bault^b

^a Normandie Univ, UNIROUEN, UNICAEN, CNRS, M2C, 76000 Rouen, France

^b BRGM, 3 av. C. Guillemin, 45060 Orleans Cedex 02, France

* Corresponding author. lisa.baulon@etu.univ-rouen.fr

Abstract

Estimating groundwater level evolution is a major issue in the context of climate change. Groundwater is a key resource and can even account in some countries for more than half of the water supply. Groundwater trend estimates are often used for describing this evolution. However, the estimated trend obviously strongly depends on available time series length, which may be caused by the existence of long-term variability of groundwater resources. In this paper, using a groundwater level database in Metropolitan France as an example, we address this issue by exploring how much trend estimates are sensitive to low-frequency variability of groundwater levels. Database consists of relatively undisturbed groundwater level time series regarding anthropogenic influence (water abstraction by either continuous or periodic pumping). Frequent changes in trend direction and magnitude are detected according to time series length, which can eventually lead to contradictory interpretations of the groundwater resource evolution, as presented in first part of this article. To assess whether low-frequency variability – known to originate from climate variability – can induce such modifications of trends, we explored in a second step the multi-time scale variability of groundwater levels using a methodology based on discrete wavelet transform. Most of the time series displaying changing trends depending on time series length corresponded to aquifers with high-amplitude low-frequency variability of groundwater levels. Two

27 predominant low-frequency components were detected: multi-annual (~7 years) and decadal (~17
28 years). We finally examined how much those two low-frequency components may affect trend estimates
29 on the longer time period available. For this purpose, we individually removed each of both components
30 from the original times series by discrete wavelet filtering and re-estimated trends in the filtered
31 groundwater level time series. The results showed that the groundwater level trends were highly
32 sensitive to the presence of any of these low-frequency components, which may then strongly influence
33 the estimated trends either by exaggerating or mitigating them. These results emphasize that i)
34 attributing the estimated trends only to climate change would be hazardous given the large influence of
35 low-frequency variability on groundwater level trends, ii) estimation of trends in hydrological
36 projections resulting from GCM outputs in which low-frequency variability is not well represented
37 would be subject to strong uncertainty, iii) a potential change in the amplitude of internal climate
38 variability – e.g. increasing or decreasing low-frequency variability – in the next decades may lead to
39 substantial changes in groundwater level trends.

40

41 **Keywords**

42 Low-frequency variability; Groundwater level trends; Metropolitan France; Maximum overlap discrete
43 wavelet transform

44

45 **1. Introduction**

46 According to Iliopoulou and Koutsoyiannis (2020), the number of scientific publications using the word
47 “trend” has steadily increased over the past two decades, especially in relation to hydroclimatological
48 variables. Various scientific questions and aims can lead scientists to search for trends in hydrological
49 processes. The assessment or forecasting of the qualitative and quantitative evolution of environmental
50 variables – such as detecting short- to long-term increases or decreases – are part of this (Visser et al.,
51 2009; Giuntoli et al., 2013; Sakizadeh et al., 2019; Caporali et al., 2020; Dudley et al., 2020). These
52 questions are related to resource preservation issues in the context of global change. For instance, the

53 European Union’s Water Framework Directive is based on this philosophy: detect negative trends in
54 water resources (streamflow and groundwater levels) with the aim of their protection (European
55 Commission, 2009); deterioration of a resource can cause restrictions on freshwater withdrawals.

56

57 In the context of climate change, assessing the long-term evolution of hydrological variables and
58 associated extremes is a major issue, particularly for identifying which parts of this evolution can be
59 attributed to climate change and to anthropogenic forcing (Massei et al., 2020). For groundwater, this
60 issue is even more relevant when considering pumping; for instance, groundwater provides 65% of the
61 water supply in France (Chataigner et al., 2019). Hence, the study of long-term groundwater level
62 evolution is especially relevant for management purposes and the knowledge of groundwater resource
63 capacity. Methods for identifying linear or monotonic trends are commonly used for describing changes
64 in hydrological variables (Stahl et al., 2010; Lorenzo-Lacruz et al., 2012; Blöschl et al., 2019; Pathak
65 and Dodamani, 2019; Vicente-Serrano et al., 2019; Mohanavelu et al., 2020; Peña-Angulo et al., 2020).

66

67 Although the detection of monotonic trends is a widely used tool for quantifying evolution of
68 hydrological variables, its use may still raise questions. First, they cannot be extrapolated to other study
69 periods, and longer or shorter periods, regardless of the type of variable considered (Koutsoyiannis,
70 2006; Burn and Whitfield, 2018). For a given region, authors commonly find contradictory or varying
71 results as trends are often not estimated over the same periods, a point that is often discussed as a major
72 issue (Hannaford et al., 2013; Degefu et al., 2019). Therefore, their “non-extrapolability” makes them
73 poor predictors and unsuitable for forecasting (Iliopoulou and Koutsoyiannis, 2020). Second, trends
74 commonly reflect long-range dependence/autocorrelations, because of low-frequency variability in the
75 hydroclimatic variables of interest (Iliopoulou and Koutsoyiannis, 2020). Such variability generated by
76 large-scale atmospheric and oceanic circulation patterns is the primary source of a “misperceived” trend,
77 as short-term periods affected by a trend may actually be part of longer-term fluctuations. Multi-
78 temporal trend-definition methods have been developed to highlight this dependence of trend
79 assessment on low-frequency variability (multi-annual–multidecadal) in hydroclimatic variables and to

80 avoid trend “misperceptions” (McCabe and Wolock, 2002; Schmocker-Fackel and Naef, 2010;
81 Hannaford et al., 2013; Stojković et al., 2014; Peña-Angulo et al., 2020). For instance, Hannaford et al.
82 (2013) demonstrated that trend direction and magnitude are highly influenced by interdecadal
83 variability.

84

85 Given the influence of interdecadal variability, and more generally low-frequency variability, on the
86 hydrological trends, it is crucial to better understand the large-scale origin of these fluctuations and how
87 catchments can filter and modify them. In this regard, Gudmunsson et al. (2011) indicated that the low-
88 frequency variability of runoff directly originates from the large-scale atmospheric circulation, while
89 the catchments properties control the proportion of variance of low-frequency variability in hydrological
90 variables. Simultaneously, a large amount of studies addressed the large-scale origins of such
91 variabilities in hydroclimatic variables (streamflow, precipitation, groundwater, temperature), using
92 climate indices and atmospheric fields (Massei et al., 2010; Boé and Habets, 2014; Dieppois et al., 2013;
93 Dieppois et al., 2016; Massei et al., 2017; Neves et al., 2019; Liesch and Wunsch, 2019).

94

95 Across the whole metropolitan France area, Fossa et al. (2021) detected ~3-yr and ~7-yr variabilities in
96 streamflow, precipitation and temperature but with fluctuating amplitudes depending on the region. At
97 a smaller regional scale, particularly in the Seine watershed, many studies previously highlighted these
98 same two low-frequency variabilities in precipitation and streamflow as well as a ~17-yr variability
99 (Massei et al., 2007; Massei et al., 2010; Fritier et al., 2012; Massei and Fournier, 2012; Dieppois et al.,
100 2013; Massei et al., 2017). The North Atlantic Oscillation (NAO) was described as one significant driver
101 of such temporal signature (~7-yr and ~17-yr) in precipitation and streamflow (Massei et al., 2007;
102 Massei et al., 2010). Later, Massei et al. (2017) highlighted using a composite analysis with Sea Level
103 Pressure (SLP) that the atmospheric pattern associated to the ~7-yr variability was not exactly
104 reminiscent of the NAO, with centers of action actually shifted to the North. Similarly, the pattern
105 associated to ~17-yr variability was a spatially extended pattern across the Atlantic ocean with lower
106 SLP roughly following the Gulf Stream front. This result highlighted that atmospheric patterns

107 associated to ~7-yr and ~17-yr variabilities are not similar and these atmospheric patterns exhibit centers
108 of action that are not necessarily corresponding to those of established climate indices such as the NAO.
109

110 Aquifers very often act as rather strong low-pass filters, leading to high-amplitude low-frequency
111 variability in groundwater levels. In other words, aquifers filter out high-frequency (short-term)
112 variations of the precipitation input more or less significantly, letting only low-frequency (longer-term)
113 variations dominate the overall variability of the groundwater level signal. Some studies also
114 investigated the role played by geological characteristics in controlling the magnitude of these
115 fluctuations in groundwater levels: thickness of superficial formations, of the vadose zone, hydraulic
116 properties of aquifers (Slimani et al., 2009; El Janyani et al., 2012; Velasco et al., 2017). In Normandy,
117 Slimani et al. (2009) and El Janyani et al. (2012) identified a significant ~7-yr variability in groundwater
118 levels of chalk aquifer consistent with many previous works that had already documented the presence
119 of both ~7-yr and ~17-yr variabilities, and their link to the NAO in northern France on precipitation
120 (Massei et al., 2007) or river flow (Massei et al., 2010, 2012, 2017). Later, the exact same multi-annual
121 and decadal fluctuations were also identified in groundwater levels in Great Britain (Rust et al., 2019)
122 and on the western European continent (Liesch and Wunsch, 2019; Neves et al., 2019).

123
124 In this article, we specifically addressed the issue of the influence of low-frequency variability on
125 groundwater level trend estimates. In metropolitan France, for instance, many changes in trend direction
126 and magnitude were observed depending on the length of time series considered, thus leading to
127 completely contradictory conclusions on groundwater level evolutions, as exposed in section 3.1. In
128 some surface hydrology studies (e.g. Hannaford et al., 2013, as mentioned previously), such
129 contradictory conclusions were related to low-frequency variability. Therefore as a second step, we
130 aimed to determine whether French aquifers concerned by these regular changes in trend direction and
131 magnitude, exhibited a significant low-frequency variability in groundwater levels. In section 3.2., we
132 thus broke down groundwater level signals using discrete wavelet transform and quantified the variance
133 percentage of total signal explained by each time scale of variability. Finally, in a third step, we
134 examined if and how low-frequency variability influenced trend estimates by filtering out each low-

135 frequency component from the original time series using discrete wavelet transform and re-estimating
136 trends on filtered time series (Section 3.3.). This last point is particularly important because if the low-
137 frequency variability significantly influences the estimated groundwater level trends, this has several
138 implications:

- 139 (i) First, regarding the identification of traces of climate change in groundwater levels. Indeed,
140 if the low-frequency variability in groundwater levels significantly affects trend estimates,
141 it is hazardous to conclude that, for instance, a decreasing evolution of groundwater levels
142 is directly the result of climate change. Indeed, such trends would then be primarily the
143 result of internal climate variability instead of anthropogenic climate change.
- 144 (ii) Second, regarding future projections. Indeed, trend estimates in hydrological projections
145 resulting from GCM outputs in which low-frequency variability is not well represented
146 would be subject to strong uncertainty.
- 147 (iii) Third, regarding future evolutions. Indeed, a potential change in the amplitude of internal
148 climate variability – e.g. increasing or decreasing low-frequency variability – in the next
149 decades may lead to substantial changes in groundwater level trends.

150

151 **2. Data and methods**

152 2.1. Data

153 2.1.1. Groundwater data

154 For this study, we used 215 boreholes in continental France, with groundwater level time series being
155 little or not affected by pumping (Fig. 1). They were selected from a BRGM database on boreholes not
156 influenced by human activities (Baulon et al., 2020) that was constituted in three steps:

- 157 (i) a selection of boreholes with time series satisfying criteria of duration, minimum amount of
158 data per month, maximum length of gaps;
- 159 (ii) the crossing of pre-selected boreholes with other BRGM databases on known anthropogenic
160 influences;

161 (iii) numerous visualisations of time series with the hydrogeologists responsible for piezometric
162 networks, in order to retain only non-influenced boreholes.

163 Time series of boreholes in this database were initially gathered in the ADES database that contains all
164 groundwater data (quantity and quality) across continental France (<https://ades.eaufrance.fr/>).

165

166 *Figure 1. Spatial distribution of the 215 little- or non-influenced groundwater boreholes in*
167 *continental France*

168

169 The criteria satisfied for selecting groundwater level time series in the database, and thus for the present
170 study, were:

- 171 • The duration of the groundwater level time series must be >30 yr for regions where monitoring
172 history is sufficiently long, and >20 yr for regions where monitoring history is shorter.
- 173 • The time series must contain a minimum amount of data in a month. This minimum amount is
174 divided into two parts. A date of sampling-frequency change is identified in each time series,
175 and the minimum sampling frequency must be at least one datum per month before this date
176 and three data per month after this date.
- 177 • The length of consecutive gaps must be <3 yr for time series starting after 1950 and <10 yr for
178 time series starting before 1950. This allows time series in the new database to preserve low-
179 frequency variability in the data. Several gaps in the time series can be allowed if these criteria
180 are respected, and if the number of gaps and their lengths are small.

181 Before data analysis, a visual check of the groundwater level time series served to remove or correct
182 erroneous data. Wishing to qualify the behaviour of water tables by including annual variability, we
183 decided to work on monthly averages. Any missing months in these time series were then filled by linear
184 interpolation, before spectral analyses.

185

186 In continental France, groundwater level time series in some regions span on a limited historical time
187 period, especially in western and southern France. Hence, we decided to focus on two different time
188 spans: 1996–2019 and 1976–2019. For all French aquifers, the analyses cover the 1996–2019 period,

189 ensuring a good trade-off between time series length and spatial coverage (215 time series available).
190 The longer period, spanning 43 years between 1976 and 2019, covered 102 time series in northern
191 France. These two periods are referred to as “reference periods”.

192

193 In our study, the selected wells are representative of the various French hydrogeological contexts:
194 alluvial, sedimentary, volcanic, and bedrock aquifers, but most wells are in sedimentary aquifers,
195 primarily in the Paris Basin, and some in the Aquitaine Basin. Each well is attached to a hydrogeological
196 area based on the groundwater bodies.

197

198 In the resulting database, the Seno–Turonian chalk aquifer of the Paris Basin is the best represented (60
199 boreholes), followed by Jurassic limestone aquifers in Lorraine, Berry, and Poitou on the rim of the
200 Paris Basin (19 boreholes), and the Eocene Beauce limestones aquifer (8 boreholes). Wells in the
201 Aquitaine Basin mainly capture the Jurassic limestone aquifer of the northern part of the Basin (7
202 boreholes) and multiple sedimentary hydrogeological formations in the southern part (sand, limestone:
203 10 boreholes). Finally, most of the wells selected in the Rhône valley monitor alluvial and fluvio-glacial
204 formations (11 boreholes).

205

206 Alluvial aquifers are also well represented in the dataset, especially the Rhine/Vosges alluvium (18
207 boreholes) in Alsace, the Garonne alluvium in the Toulouse region (3 boreholes), and recent alluvium
208 in the Mediterranean region (11 boreholes).

209 Some wells in the Central Massif are located in volcanic aquifers in various formations with different
210 behaviour of groundwater levels (5 boreholes). Finally, bedrock aquifers are monitored by a few selected
211 wells in the Armorican Massif (10 boreholes).

212

213 2.1.2. Precipitation data

214 Precipitation data used in this study come from the SAFRAN reanalysis (Vidal et al., 2010), which
215 provides daily data on an 8×8 km² mesh covering France from 1958 to 2019. In addition, based on

216 meteorological data (precipitation (P), snow, temperature, and Penman-Monteith potential
217 evapotranspiration (PET)) from the SAFRAN reanalysis, effective precipitation ($EP = P - PET$) data
218 were computed using a gridded water-budget model with 8 km resolution at a daily time step, relying
219 on the water-budget method of Edijatno and Michel (1989). The water-budget method considers that
220 in the water cycle, the soil acts as a reservoir characterized by its water storage capacity. Edijatno and
221 Michel (1989) introduced a quadratic law to progressively empty the soil water reserves and to distribute
222 the positive difference between P and PET between EP and soil storage. In the present study, the
223 temporal resolution of both precipitation and effective precipitation was set at a monthly time step by
224 using monthly cumulated data.

225

226 2.2. Methods

227 2.2.1. Trends over multiple time series lengths

228 We first estimated groundwater level trends over multiple time series lengths. We then determined
229 whether changes in the length of time series affected trend estimates, by assessing the stability of trends
230 when comparing the direction and magnitude of trends over decreasing periods. The procedure is
231 illustrated in Fig. 2a. As explained above, we split the trend stability analysis into two reference periods,
232 1976–2019 and 1996–2019, corresponding to the best agreements between the spatial distribution of
233 wells and groundwater level time series lengths over northern aquifers (102 boreholes) and all of
234 continental France (215 boreholes), respectively. The 1996–2019 reference period provided an image
235 of the stability of groundwater level trends through whole continental France, though over a relatively
236 short period. To improve the consistency of the study, the 1976–2019 reference period was used for
237 obtaining a longer historical hindsight, but covering only northern aquifers due to the data availability.

238

239 **Figure 2.** Workflow of (a) trend stability analysis over decreasing time periods and (b) assessment of
240 groundwater low-frequency influence on trend direction and magnitude. “WLF” is “water level
241 fluctuation”.

242

243 To complete the stability analysis, we first evaluated the magnitude of trends and their statistical
244 significance over different study periods (Fig. 2a; Step 1). Within the 1976–2019 reference period,
245 trends were estimated for all groundwater level time series over six periods: 1976–2019, 1981–2019,
246 1986–2019, 1991–2019, 1996–2019 and 2000–2019. Within the 1996–2019 reference period,
247 groundwater level trends were estimated over two study periods: 1996–2019 and 2000–2019. The
248 significance of monotonic trends was determined with a modified Mann–Kendall trend test for
249 autocorrelated data (Hamed and Ramachandra Rao, 1998). Compared to the well-known Mann–Kendall
250 trend test (Mann, 1945; Kendall et al., 1987), the modified Mann–Kendall trend test considers
251 autocorrelation by correcting probability values (p-values) after accounting for autocorrelation. The
252 threshold for statistical significance was set at 5%. As we primarily aimed at quantifying changes in
253 groundwater level trends in relation to groundwater stock variation over decreasing time periods – which
254 cannot be estimated by the significance value of the modified Mann–Kendall trend test – we developed
255 an indicator describing this phenomenon. Therefore, although the statistical significance of trends was
256 also tested in the present study, we decided to present only the afore-mentioned indicator.

257

258 To develop this indicator, we first assessed the magnitude of trends by estimating Sen’s slope (Sen,
259 1968), this method was selected as it is less sensitive to outliers than linear regression. The slope is
260 defined as the median of the set of slopes calculated between pairs of points. To evaluate the relative
261 importance of trends, compared to the groundwater stock variation, the percentage of decrease or
262 increase in groundwater levels compared to the maximum water level fluctuation (WLF) was calculated
263 using the following equation:

$$264 \quad \text{Percentage of maximum WLF} = \left(\frac{\text{Sen's slope} * \text{duration}}{\text{Maximum WLF}} \right) * 100 \quad (1)$$

265 where maximum WLF is the difference between the highest and the lowest groundwater levels measured
266 for a given time series. This normalisation of Sen’s slope by the maximum WLF allowed comparing the
267 magnitude of groundwater trends between aquifers with various water table behaviours and significant
268 differences in their water stock variations.

269

270 The percentages of groundwater level loss/gain against maximum WLF were split into five classes
271 according to their magnitude:

- 272 • Negligible trends between -1% and +1% of maximum WLF;
- 273 • Moderate upward or downward trends between +1% and +10%, or -1% and -10%, of the
274 maximum WLF, respectively;
- 275 • Strong upward or downward trends between +10% and +100%, or -10% and -100%, of the
276 maximum WLF, respectively.

277 This normalisation was applied to every well for each period analysed. The maximum WLF adopted,
278 i.e. that of the two reference periods, remained constant from one period to the next, as it is a parameter
279 that we used for characterising the groundwater stock variation.

280

281 For each well, the trend stability was evaluated by comparing the trend direction and belonging to the
282 above classification for all studied periods (Fig. 2a; Step 2). For a given borehole, the groundwater trend
283 can be stable or unstable in direction. We considered a trend direction “stable” if its direction was
284 constantly upward, downward, or negligible from one period to another. Conversely, a trend was
285 “unstable” when its direction fluctuated depending on the study period, or whether a trend emerged,
286 such as a negligible trend for a given period followed by an upward or downward trend for the next
287 period. Moreover, a “direction-stable” trend can be stable or unstable in magnitude; it is stable when the
288 magnitude class does not change between periods and unstable if it does change.

289

290 2.2.2. Groundwater multi-timescale variability analysis

291 To determine the importance of low-frequency variability in groundwater levels, we identified and
292 extracted high- to low-frequency wavelet components by multiresolution analysis, using the maximum
293 overlap discrete wavelet transform (MODWT) algorithm. Like the more common discrete wavelet
294 transform (DWT) method, MODWT is an iterative filtering of time series using a series of low- and
295 high-pass filters, producing one high-frequency component, or “wavelet detail”, and one lower
296 frequency component called “approximation” or “smooth” at each scale. The smooth component is then

297 further decomposed into a wavelet detail and a smooth component, the latter being decomposed again
298 until it can no longer be decomposed. The original signal can be reconstructed by summing up all the
299 wavelet details and the last smooth. The original signal is then separated into a relatively small number
300 of wavelet components from high to low frequencies, which together explain the total variability of the
301 signal. For this study, the maximum decomposition level used in the MODWT was $\log_2(N)$ where N is
302 the length of the time series. The least-asymmetric (symmlet) wavelet “s20” was used in order to better
303 capture variability at all time scales of sometimes relatively smooth groundwater level time series.

304

305 However, unlike DWT, MODWT was essentially designed to prevent phase shifts in the transform
306 coefficients at all scales by avoiding downsampling – reducing by a factor 2 the number of coefficients
307 – the signal with increasing scales. It results that the computed wavelet and scaling coefficients at each
308 scale remain aligned with the original time series; that is, the variance explained by these coefficients is
309 located where it truly lies in the time series analysed (Percival and Walden, 2000; Cornish et al., 2003;
310 Cornish et al., 2006). While not necessarily essential for signal or image processing or numerical
311 compression, this property is fundamental for physical interpretation of the wavelet details in
312 multiresolution analysis, and has already been used to that purpose in several studies such as Percival
313 and Mofjeld (1997), Massei et al. (2017) and Pérez Ciria et al. (2019).

314

315 The dominant frequency associated with each MODWT wavelet detail was calculated by Fourier
316 transform of each wavelet detail. The MODWT also provides the amount of variance (or energy)
317 explained by each wavelet detail and frequency level. The energy percentage of a given wavelet detail
318 expresses the relative importance of this variability in the total signal variability. As a result, the energy
319 distribution between wavelet details for each well in the database can be extracted and mapped.

320

321 Continuous global wavelet spectra were also calculated by averaging the spectral power from the
322 continuous wavelet spectra over time (Torrence and Compo, 1998). These analyses used R packages
323 *wmtsa* (Constantine and Percival, 2016) and *biwavelet* (Gouhier and Grinsted, 2012). They were
324 conducted for both reference periods: 1976–2019 and 1996–2019.

325
326
327
328
329
330
331
332
333
334
335
336
337
338
339
340

2.2.3. Influence of low-frequency variability of groundwater levels on trend direction and magnitude

The influence of groundwater low-frequency variabilities on the trend direction and magnitude was estimated using the MODWT method. As described in Section 2.2.2., summing up all wavelet details and the last smooth rebuilds the original signal. Based on this assessment, we first subtracted the wavelet detail of interest (or component) corresponding to a specific variability from the original signal (i.e., groundwater level monthly averages) (Fig. 2b; Step 1). We then calculated the Sen’s slope (Section 2.2.1.) of the filtered signal and normalised it to the maximum WLF of the original signal (i.e., without filtering) (Fig. 2b; Step 2). The interest in keeping a fixed maximum WLF to normalise Sen’s slopes is to assess only the influence of the removal of the component on the slope, and not to assess the influence of the removal of the component combined to variance modification linked to the removal of the component. Finally, we compared the magnitude and direction of the trends between the original and filtered signals to assess the influence of the component on the trend of the original signal. This analysis covered both reference periods: 1976–2019 and 1996–2019.

341 **3. Results**

342 **3.1. Stability of trend directions and magnitudes of groundwater levels**

343 In this section, we investigate the stability of groundwater level trends, that is, we aim at determining if
344 trend direction and magnitude change according to the length of time series used for the trend analysis.
345 To this end, we introduce the notions of “trend stability” (no change in direction or magnitude) and
346 “instability” (changes in direction or magnitude) over decreasing time periods. If trend direction is
347 stable, we consider that the length of time series has a minor influence on trend estimate, then a
348 conclusion about groundwater level evolution may be drawn. Conversely, if it is unstable, the time series
349 length has a significant influence on such estimate, then any conclusion regarding groundwater level

350 evolution may not be drawn. The trend-stability maps for the reference periods (1976–2019 and 1996–
351 2019) used to verify this hypothesis, are shown on Figure 3.

352

353 **Figure 3.** *Trend-stability maps from the two reference periods (a) 1976–2019 to 2000–2019 and (b)*
354 *1996–2019 to 2000–2019. These maps show for a given reference period to what extent groundwater*
355 *level trends are susceptible to changes of direction and magnitude according to the time series length.*
356 *If the change of time series length does not affect trend direction (stable trend in direction), a triangle*
357 *or a square is drawn for the borehole. If the change of time series length affects trend direction*
358 *(unstable trend in direction), a diamond or a crossed-out circle is drawn according the type of trend*
359 *instability. Finally, if the change of time series length does not affect trend magnitude (stable trend in*
360 *magnitude), a dot is added in the symbol.*

361

362 From the 1996–2019 reference period, some hydrogeological formations show an instability in trend
363 direction (positive and negative trend; Fig. 3b). These instabilities in trend direction are represented on
364 maps either with a diamond in case of change of sign from a period to another period (alternating positive
365 and negative trend) or a crossed-out circle in case of emerging trend (insignificant trend and positive or
366 negative trend). These entities are the Eocene Beauce limestones, the Seno–Turonian chalk of Artois–
367 Picardy (Fig. 4; Beauval), and the Jurassic limestones from Sarthe to Bessin. For these entities, no
368 conclusions regarding the evolution of groundwater levels can be drawn, given the recurrent change in
369 trend direction according to the length of time series taken into account for the trend analysis.

370

371 **Figure 4.** *Example of trends over multiple time series lengths (1996–2019 and 2000–2019) on*
372 *monthly groundwater levels at Beauval (Seno-Turonian chalk of Artois-Picardy), Goupillières (Seno-*
373 *Turonian chalk of Normandy/Picardy) and Penol (fluvio-glacial formations in Rhône valley).*

374

375 Conversely, the Seno–Turonian chalk of Normandy/Picardy (Fig. 4; Goupillières), the Jurassic
376 limestones of Poitou and Berry, the fluvio-glacial formations of the Rhône valley (Fig. 4; Penol), the
377 Brittany bedrock, Champagne and Bourgogne chalk exhibit stable trend directions (Fig. 3b). For these

378 entities, conclusions regarding groundwater level evolution may be drawn: they are still downward
379 regardless the study period.

380

381 However, if the analysis is conducted over longer periods for hydrogeological entities of northern France
382 (particularly for the Normandy/Picardy, Champagne and Bourgogne chalk), changes in trend direction
383 or a trend emergence can be detected when changing the time series length (Fig. 3a). Consequently,
384 conclusions regarding the groundwater level evolution drawn for the 1996–2019 reference period are
385 no longer valid for the 1976–2019 reference period since instabilities in trend direction are detected.
386 Naturally, boreholes with trend direction instability between 1996–2019 and 2000–2019 periods are also
387 subject to this instability over longer periods. Overall, the result is not homogeneous within the same
388 hydrogeological unit as we can detect both boreholes with stable and unstable trend directions.

389

390 Most boreholes with stable (upward or downward) trend directions from the shorter reference period
391 (1996–2019) are also stable in magnitude, meaning that the importance of slope in relation to
392 groundwater level amplitude does not change class (Fig. 3b – dot in the symbol). This is the same for
393 the longer reference period (1976–2019) in the western Seno-Turonian chalk of Normandy and the
394 Lutetian/Ypresian sands of the Paris Basin (Fig. 3a).

395

396 Overall, when stable trend directions are detected, from the reference period 1976–2019 for northern
397 France and 1996–2019 for the other regions of France, and that conclusions on groundwater level
398 evolutions can be drawn, the levels are in the majority decreasing (Fig. 3). The existence of unstable
399 trend directions raises the following question: are there low-frequency variabilities in groundwater
400 levels that could induce these changes in trend directions and thus influence the trend estimates?
401 Consequently, next section aims to identify the existence and significance of low-frequency variability
402 in groundwater level signals.

403

404 3.2. Groundwater level fluctuations across multiple timescales: significance and spatial 405 distribution over France

406 In this section, we assess the existence, significance and spatial distribution of low-frequency variability
407 in groundwater level signals over France. We aim at determining if the unstable trend directions
408 previously identified, could be potentially induced by the existence of low-frequency variability in
409 groundwater level signals.

410

411 The energy percentage (i.e., the proportion of the total variance) at each timescale of variability can be
412 extracted via MODWT and mapped for each groundwater time series. Figure 5 shows the spatial
413 distribution of the energy contained in each spectral component, as a function of the hydrogeological
414 entity. Multi-annual (5–12 yr) and decadal (12–24 yr) variabilities dominate over much of the Paris
415 Basin (from Beauce limestones to the Seno–Turonian chalk farther north). Elsewhere, low-frequency
416 variability can also prevail over a short period (1996–2019), such as in the fluvio-glacial formations of
417 the Rhône basin, the Jurassic limestones of Poitou, and the alluvial formations of the Garonne River.
418 Increasing the length of the studied period (1976–2019) highlights the prevalence of decadal variability
419 (12–24 yr) in groundwater levels in the Beauce limestones and in the southern Seno–Turonian chalk of
420 Normandy. This decadal variability also occurs in significant proportions farther north in the Seno–
421 Turonian chalk of Normandy, but there its proportion is rather similar to that of the multi-annual
422 variability (5–12 yr). These observations highlight the inertial nature of water tables in Normandy chalk
423 and Beauce limestones aquifers (Fig. 6a and 6b) due to their highly capacitive nature, particularly in
424 plateau areas (Roux, 2006). In these hydrogeological units, groundwater levels depend essentially on
425 recharge from past winters. They are particularly sensitive to a succession of dry or wet winters, due to
426 the memory effect linked to the regulation power of the water table. Regeneration of the water table
427 stock spans several successive years with excess winter recharges.

428

429 **Figure 5.** *Proportion of the total variance explained by each timescale of variability (energy*
430 *associated to each timescale, expressed as the percentage of total energy of each groundwater time*
431 *series).*

432
433 **Figure 6.** *Examples of groundwater level time series representative of each major water tables*
434 *behaviour.*

435
436 Although these low-frequency variabilities (multi-annual and decadal) are substantial components of
437 the total groundwater variability in the Seno–Turonian chalk of the Artois–Picardy region, the annual
438 variability explains a larger part of the total groundwater variability than in Normandy and Picardy (Fig.
439 5). The groundwater levels on the borders of the Seno–Turonian chalk (Champagne and Bourgogne)
440 also display this type of variability, but here the annual variability dominates. Jurassic limestones on the
441 edge of the Paris Basin from the Lorraine region to the Berry region also show this predominant annual
442 variability with only a small part of the total variability explained by multi-annual and decadal
443 variabilities. Overall, the water tables in these hydrogeological units show a combined behaviour:
444 variously significant multi-annual to decadal variability is superimposed by prominent annual variability
445 (Fig. 6c and 6d). In these aquifers, the annual variability is all the more important as their storage
446 capacity decreases, with increasing fracturing, permeability, and proximity to the outlet (Roux, 2006).
447 Here, groundwater levels strongly depend on infiltrated rainfall during the previous winter, while having
448 a memory effect linked to the regulation power of water table.

449
450 Annual variability generally becomes predominant in compact highly fractured and low capacitive
451 sedimentary aquifers (Roux, 2006), such as the fissured Jurassic limestones of the northern Aquitaine
452 Basin or in fractured bedrock of Brittany (Fig. 5b and 6e). In such settings, groundwater levels rapidly
453 rise in response to winter rainfall, but drop as rapidly as soon as water input stops.

454
455 No typical pattern in the energy distribution is noticeable for alluvial aquifers in France, and the
456 dominance of one variability compared to another strongly depends upon the local geological and

457 hydrological context (Fig. 5). Boreholes monitoring alluvial formations commonly also monitor the
458 underlying water body in the absence of an impermeable layer. Consequently, the borehole captures the
459 behaviours exhibited by both groundwater bodies. Hence, water tables in alluvial formations can exhibit
460 either an annual, multi-annual, or combined behaviour.

461
462 Hydrogeological entities previously described as susceptible to trend direction instabilities, are
463 essentially entities for which the water tables display inertial or combined behaviour, which means that
464 the existence of a low-frequency variability in groundwater levels and in significant proportions could
465 be partly responsible for these instabilities (Fig. 3 and 5). These entities are: the Normandy/Picardy
466 chalk, the Artois-Picardy chalk, the Bourgogne and Champagne chalk, the Beauce limestones, and the
467 southern Jurassic limestones from Sarthe to Bessin.

468
469 The superposition of all the global wavelet spectra calculated for each groundwater level time series
470 gives us a synthetic view of the predominant variabilities in groundwater levels of French aquifers (Fig.
471 7). The three preeminent variabilities in monthly groundwater levels are: ~1 yr, 5–8 yr (~7-yr), and >12
472 yr (~17-yr). The ~7-yr and ~17-yr variabilities show larger spectral powers and carry the largest part of
473 the low-frequency variability in monthly groundwater levels. Such characteristic variabilities are known
474 to be induced by large-scale climatic circulation, including the NAO, and was earlier observed in
475 Normandy groundwater levels by Slimani et al. (2009) and El Janyani et al. (2012), and in streamflow
476 of the Seine River (Massei et al., 2010). Later, studies highlighted these variabilities in groundwater
477 levels in other countries (Rust et al., 2019; Liesch and Wunsch, 2019; Neves et al., 2019).

478
479 **Figure 7.** *Global wavelet spectra of (a) 102 monthly groundwater levels over 1976–2019, covering*
480 *northern France and (b) 215 monthly groundwater levels over 1996–2019, covering all of France.*

481 *Leading variabilities are highlighted.*

482
483 Since the low-frequency variabilities significantly explain groundwater level variability, the next section
484 seeks to determine if, how and to what extent they influence the estimated trends on the reference

485 periods. As the ~7-yr and ~17-yr variabilities appear to be the predominant low frequencies in
486 groundwater level signals, hereafter, we provide details on the influence of these two variabilities on
487 groundwater level trends.

488

489 3.3. Influence of groundwater level low-frequency variability on trend direction and 490 magnitude

491 In this section, we aim at determining the influence of groundwater multi-annual (~7-yr) and decadal
492 (~17-yr) variabilities on the estimated trends. In other words, we want to determine whether these low-
493 frequency variabilities affect trend estimates, and if so, whether they aggravate or mitigate the estimated
494 trends on the reference periods. To this end, we individually removed the detected low-frequency
495 components corresponding to multi-annual and decadal variabilities and recomputed the trends for the
496 resulting filtered groundwater level signals, to assess the effect of such low-frequency components on
497 trend magnitude and direction. Low-frequency components to be filtered were chosen based on global
498 wavelet spectra (Fig. 7). For the 1996–2019 reference period, only the ~7-yr component was filtered
499 from monthly groundwater levels, while for the 1976–2019 reference period, both ~7-yr and ~17-yr
500 components were individually filtered (Fig. 8 and 9).

501

502 **Figure 8.** Comparison of groundwater trend magnitude between monthly groundwater levels and ~7-
503 yr filtered groundwater levels over 1996–2019.

504

505 **Figure 9.** Comparison of groundwater trend magnitude between monthly groundwater levels, ~7-yr
506 filtered groundwater levels, and ~17-yr filtered groundwater levels over 1976–2019. The legend of
507 hydrogeological entities can be found on Fig. 8.

508

509 Figures 8 and 9 show the magnitude of the trend (Sen's slope/maximum WLF ratio) of each groundwater
510 time series analysed. Monthly groundwater levels are in red, the ~7-yr filtered monthly groundwater
511 levels in grey, and the ~17-yr filtered groundwater levels in blue (only for the 1976–2019 period). Both

512 figures show the impact of removing a given variability (~7-yr or ~17-yr) on the trend, compared to the
513 unfiltered groundwater levels; they also show the influence of a given low-frequency variability on
514 unfiltered groundwater level trends by considering the sign of the subtraction between unfiltered (red)
515 and filtered (grey or blue) groundwater levels. Nevertheless, quantifying the exact contribution of a
516 given variability to unfiltered groundwater level trends is difficult because other (low- or high-
517 frequency) variabilities can modulate this contribution.

518

519 For the shorter period (1996–2019), the effect of the ~7-yr variability on trends shows a well-established
520 spatial pattern throughout France (Fig. 8). In the North, for aquifers with inertial or combined behaviour
521 of water tables, the ~7-yr variability drives levels up. In contrast, in various southern French aquifers,
522 this variability drives groundwater levels down.

523

524 In northern France in chalk, sands, and Eocene limestones of the Paris Basin, we see an accentuation of
525 downward trends (Fig. 10b; Goupillières), a mitigation of upward trends, and reversals in direction from
526 upward to downward trends when the ~7-yr variability is filtered from monthly groundwater levels (Fig.
527 8b1). This effect of removing the ~7-yr variability means that in unfiltered original groundwater levels,
528 this variability drives groundwater levels upward. In other words, the ~7-yr variability mitigates
529 downward trends and accentuates upward trends. The Seno-Turonian chalk of Champagne is the only
530 one not displaying this phenomenon. Around the hydrogeological entities of the Paris Basin, the effect
531 of the ~7-yr variability on groundwater levels is more sporadic.

532

533 **Figure 10.** *Typical patterns of low-frequency variability removal influence on groundwater level trend*
534 *estimates: (a) Analysis of the 1976–2019 period at Goupillières (Seno-Turonian chalk of Normandy*
535 *and Picardy) and Beauval (Seno-Turonian chalk of Artois-Picardy) both in northern France; (b)*
536 *Analysis of the 1996–2019 period at Goupillières (northern France) and Penol (southern France –*
537 *fluvio-glacial formations of Rhône valley).*

538

539 In southern France, we see a reverse pattern from that found in the North (Fig. 8). Here, removing the
540 ~7-yr variability mitigates downward trends (Fig. 10b; Penol), or results in downward trends becoming
541 upward trends (Fig. 8b2). This pattern is observed in all southern hydrogeological units analysed, even
542 if locally the removal of the ~7-yr variability may have no effect on the trends. This “non-effect” could
543 be caused either by the fact that the ~7-yr variability does not, or weakly explain, the variability of
544 monthly groundwater levels, or because this variability does not contribute to the trend at all. Overall,
545 the ~7-yr variability drives groundwater levels down in most southern hydrogeological entities. In other
546 words, the ~7-yr variability aggravates downward trends.

547

548 A transitional section between northern and southern patterns can be seen in the Jurassic limestones of
549 Berry (Fig. 8). Here, the ~7-yr variability can drive groundwater levels upward or downward. This
550 transition zone could be attributed to either a transitional climatic zone, or a high spatial variability in
551 water table behaviour, related to a spatial discrepancy of aquifer properties.

552

553 The ~7-yr variability displays a similar pattern for the longer period (1976–2019) as for the shorter one
554 in the Paris Basin (Fig. 9b). Removing this variability still results in accentuated downward or mitigated
555 upward trends. The main discrepancy compared to the shorter period is due to the fact that, in many
556 cases, removing the ~7-yr variability hardly affects the trend (Fig. 10a; Goupillières and Beauval).
557 Hence, the ~7-yr variability either drives groundwater levels upward, so mitigates downward trends, or
558 has no effect on the trend in the Paris Basin. The Seno–Turonian chalk of Champagne also displays this
559 pattern, while the Upper Cretaceous chalk of Bourgogne does not.

560

561 The long reference period allows for a robust assessment of the influence of the ~17-yr variability on
562 groundwater trends (Fig. 9), as it shows a consistent pattern in hydrogeological units of northern France,
563 driving groundwater levels downward, so aggravating downward trends. The removal of this variability
564 leads to mitigation of downward trends (Fig. 10a; Goupillières), accentuation of upward trends, or
565 reversals in trend directions from downward to upward. The only hydrogeological unit where the ~17-

566 yr variability does not influence the trend is the Seno–Turonian chalk of Artois–Picardy (Fig. 10a;
567 Beauval).

568

569 Figure 10a also shows the importance of the ~17-yr variability weakening since the late 2000s in
570 carrying trend: the trend is largely mitigated when this variability is removed from the monthly
571 groundwater levels at Goupillières. At Beauval, this is not the case, because the ~17-yr variability only
572 accounts for a small part of total variability, and therefore has no influence on the trend.

573

574 The degree of influence of a specific variability on the trend can be related to two factors: (i) the
575 proportion of total groundwater variability explained by this variability and (ii) the length of the time
576 series. The greatest influence on trends of removing a specific variability occurs when it accounts for a
577 large part of the total groundwater variability. This phenomenon is particularly remarkable in inertial
578 formations. For instance, removing the ~7-yr variability over the 1996–2019 period strongly affects
579 groundwater level trends in Beauce limestones, Seno–Turonian chalk, and fluvio-glacial formations in
580 the Rhône valley (Fig. 8). As seen earlier, the ~7-yr variability explains much of the total groundwater
581 variability in these units over the 1996–2019 period (Fig. 5b).

582

583 Similarly, removing the ~17-yr variability over the 1976–2019 period strongly affects groundwater level
584 trends in Beauce limestones and southern Seno–Turonian chalk of Normandy (south of the Seine River),
585 while this influence weakens farther north until it no longer affects trends in the Seno–Turonian chalk
586 of Artois–Picardy (Fig. 9). This weakening pattern corresponds to a decrease in the significance of the
587 ~17-yr variability in monthly groundwater variability from the Beauce limestones to the Seno–Turonian
588 chalk of the Artois–Picardy basin farther north (Fig. 5a).

589

590 In addition to the explanatory variance, the other major factor that affects the importance of a given
591 variability removal on trends magnitude and direction is the length of the time series. Thus, removing
592 the ~7-yr variability over a long period (1976–2019) has less influence on trends than over a shorter
593 period (1996–2019). We see an example of this in the northern part of the Seine River, in the Seno–

594 Turonian chalk of Normandy. During the 1976–2019 period, the ~7-yr variability still explains half of
595 the groundwater level variability (Fig. 5a), but its removal from groundwater levels hardly affects trends
596 (Fig. 9).

597

598 **4. Discussion**

599 In this section, we discuss the different items addressed in the section 3. First, we discuss how the length
600 of groundwater time series can influence trend estimation and thus conclusions regarding groundwater
601 level evolution. We also discuss to what extent it may be related to the presence of low-frequency
602 variability in groundwater signals, and to what extent the length of groundwater time series is a key
603 parameter to determine the trend origin. By trend origin, we refer to the physical phenomenon that leads
604 to the groundwater level trend. Second, we discuss the presence of low-frequency variability in
605 groundwater levels and the relationship with aquifer and catchments properties. Finally, we discuss the
606 influence of multi-annual and decadal variabilities on groundwater trends and compare these results to
607 those obtained for (effective) precipitation with the aim to determine whether these influences originate
608 from precipitation or whether catchment and aquifer properties disrupt these influences. Furthermore,
609 we develop the implications of such results on the interpretation of estimated groundwater level trends
610 as well as on future evolutions and projections of groundwater levels.

611

612 **4.1. Importance of time series length on trend estimates and to discuss the origin of** 613 **groundwater trends**

614 A few studies have previously examined the influence of time series length on the magnitude and
615 statistical significance of hydroclimatic variable trends. It emerged that the shorter the study period, the
616 greater its magnitude and statistical significance, which appeared to be directly linked to low-frequency
617 variability (Hannaford et al., 2013; Peña-Angulo et al., 2020). The low-frequency variability also
618 interferes in the statistical test results with high magnitude trends that may be statistically insignificant
619 but may actually have important implications for water resources (Morin, 2011; Fatichi et al., 2015a).

620 The main method for mitigating the effect of multi-annual and multidecadal variabilities on trends is to
621 lengthen the study period as much as possible (Peña-Angulo et al., 2020). However, the main limitation
622 to lengthen the study period comes from the existence of historical data. In our case, the French
623 piezometric network is relatively young, which constrains trend studies to be realised on short periods.
624 Therefore, as much studies (Burn et al., 2012), our trend study is conducted using temporal windows
625 that provide the best compromise between time series length and the spatial coverage of *in situ* stations.

626

627 We showed that some aquifers exhibiting inertial or combined behaviour of water tables are particularly
628 susceptible to trend direction instabilities (alternatively upward and downward) when the length of
629 groundwater time series is modified. It is therefore difficult to draw a conclusion on the groundwater
630 level evolution. Shifting trend directions are not specifically inherent to groundwater levels but can also
631 be observed in streamflow and precipitation (Hannaford et al., 2013; Stojković et al., 2014; Espinosa
632 and Portela, 2020; Peña-Angulo et al., 2020). Such trends should be interpreted with great care, as they
633 may actually correspond to the presence of low-frequency variability, and do not represent a physically
634 meaningful trend behaviour, i.e., a change in the behaviour of the analyzed phenomenon that may
635 eventually lead to a new (yet unknown) state, for instance as a consequence of anthropogenic climate
636 change or changes in land use.

637

638 However, the existence of significant low-frequency variability in groundwater levels does not
639 necessarily induce trend direction instabilities, as it was observed for some aquifers exhibiting water
640 tables with inertial or combined behaviour. In such case with still upward or downward trends regardless
641 the time series length, conclusions about groundwater level evolution may be drawn. Nevertheless,
642 observing still upward or downward trends does not allow us to deduce the origin of the trend. For
643 instance, the detected decreasing trends may be induced either by (i) the anthropogenic climate change
644 resulting in a decrease in groundwater recharge, (ii) the internal climate variability (developed in
645 subsequent paragraphs), or (iii) anthropogenic impacts (e.g., groundwater pumping, changes in land
646 cover that may generate a decrease in groundwater recharge).

647

648 Internal climate variability (i.e. the low-frequency variability) may lead to stable trend directions in
649 different ways according our observations (not exhaustive). First, since low-frequency variability
650 displays an aperiodic behaviour with regular amplitude-modifications, consequently trends may be
651 largely guided by these amplitude-modifications of low-frequency that may lead to a trend direction still
652 upward or downward regardless the length of time series considered (developed in Section 4.3.). Second,
653 trends detected over relatively short periods may actually be only sections of slower fluctuations.
654 Consequently, the trend direction remains upward or downward regardless the time series length
655 considered, since the available length of groundwater level time series is still too short to grasp certain
656 low-frequency timescales as fluctuations, but they are grasped to be trends. So, these trends which over
657 short study periods, without caution, would be imputed easily to climate change may actually only be
658 sections of slower fluctuation (from internal climate variability) that cannot be evidenced by the length
659 of the study period. Because large-scale atmospheric and oceanic fluctuations are expressed over a wide
660 range of timescales, any groundwater trend could be the result of a slower fluctuation (Rossi et al.,
661 2011). For instance, the Atlantic Multidecadal Oscillation (AMO) oscillates on ~60-yr timescales (Kerr,
662 2000; Enfield et al., 2001). As mentioned earlier, the age of French piezometric networks does not, in
663 most cases, allow us to grasp such a low-frequency timescale as a fluctuation in groundwater levels, but
664 it can be grasped to be trend. To overcome these drawbacks, some studies have used the Ensemble
665 Empirical Mode Decomposition (EEMD) method to filter out climate variability in precipitation,
666 streamflow, or meteorological drought signals and detect non-linear trends (Massei and Fournier, 2012;
667 Sang et al., 2014; Guo et al., 2016; Song et al., 2020). For instance, Massei and Fournier (2012)
668 concluded that the non-linear trend in the daily Seine River flow could be related to a larger scale NAO
669 fluctuation, indicating the reversibility of the phenomenon. Therefore, this highlights the complexity to
670 define whether the trends in hydroclimate variables can be related to climate change or are simply a
671 portion of some low-frequency fluctuations of large-scale atmospheric or oceanic circulation.

672

673 Without considering the anthropogenic impacts (which data are often poorly referenced), the most
674 limiting factor for distinguishing a climate change origin of the trend from an internal climate variability
675 origin (in particular from segments of low-frequency fluctuations that may appear as short-term trends)

676 remains the availability of groundwater level data. Studies on groundwater level reconstruction might
677 overcome this constraint via, for instance, deep learning approaches or tree-ring-based reconstructions
678 (Vu et al., 2020; Tegel et al., 2020). However, disentangling climate change and large-scale climate
679 natural variability would still remain difficult, even with longer time series data, as anthropogenic
680 forcing may have already impacted climate variability (Dong et al., 2011; Caesar et al., 2018).

681

682 Disentangling the determinism of trends in terms of internal climate variability or climate change lies
683 behind the scope of the present study. It is rather dedicated to assess how low-frequency variability can
684 affect trend estimations. Owing to the database used, the trends possibly detected here cannot result
685 from groundwater abstraction by pumping. However, as this database does not consider changes in land
686 cover, some trends in groundwater levels could then result from such influence involving recharge
687 modifications for instance.

688

689 4.2. Catchment and aquifer properties and their impact on variability time scales of 690 groundwater levels

691 The analysis of the spatial distribution of multi-timescale variability revealed the predominance of ~1-
692 yr, ~7-yr, and ~17-yr variabilities in groundwater levels throughout Metropolitan France. The ~1-yr
693 variability can be explained by the hydrological cycle (winter recharge and summer recession), while
694 the ~7-yr and ~17-yr variabilities originate from climatic/oceanic large-scale variability as already
695 demonstrated by Massei et al. (2010), Massei and Fournier (2012), El Janyani et al. (2012) or more
696 recently Rust et al. (2019).

697

698 The present study showed that the significance of the low-frequency variability in groundwater levels
699 is highly variable between French hydrogeological entities. The low-frequency variability can be either
700 predominant in the total variance of groundwater levels or weakly depicted. These discrepancies are
701 primarily dependent on intrinsic catchment and aquifer properties such as the permeability and thickness
702 of the unsaturated zone, the hydrodynamic properties (transmissivity and storage coefficient), the

703 aquifer geometry, the connection with neighbouring aquifers and river system (El Janyani et al., 2012;
704 Rust et al., 2018).

705

706 Aquifers constituted of rocks with low matrix porosity and highly fractured such as limestones and
707 bedrock would tend to exhibit groundwater levels dominated by an annual variability and a weak low-
708 frequency variability due to a high diffusivity. Conversely, aquifers with high storage capacity and
709 thickness, low transmissivity, and significant thickness of superficial formations such as chalk aquifers
710 tend to display groundwater levels dominated by multi-annual to decadal variabilities (Slimani et al.,
711 2009; El Janyani et al., 2012). The exact same behaviour was also recently highlighted by Rust et al.
712 (2019) in chalk aquifers of Great Britain.

713

714 However, the location in the regional geomorphology (valley, plateau) and hydraulic gradient would
715 exert a strong control on the significance of multi-annual and decadal variabilities in groundwater levels
716 (El Janyani et al., 2012), with high-amplitude low-frequency variations for downgradient piezometers.
717 On the contrary, piezometers with lower amplitudes of low-frequency variations and high amplitudes
718 of annual variations would be generally found at upgradient locations and then not associated to the
719 drainage of large areas of subterranean watersheds. Such boreholes would then also be located on
720 plateau areas, where superficial formations and unsaturated zone are thinner (Slimani et al., 2009). It
721 then turns out that the geomorphological context and properties such as the presence of superficial
722 formations, aquifer thickness and transmissivity, but also the location within the hydraulic gradient are
723 determinant explanatory factors.

724

725 Local conditions would also play a major role in defining the hydrogeological determinism of
726 groundwater level behaviour. For instance, piezometers located downgradient would correspond to the
727 drainage of a large volume of aquifer and would then display enhanced low-frequency behaviour, but
728 in karst areas such boreholes are also very likely associated to highly transmissive karst zones (the so-
729 called “output karst”) that display strong and fast response to precipitation (i.e., favoring high amplitude
730 high-frequency variations). The influence of such characteristics on the frequency behaviour of

731 groundwater levels have been successfully put in evidence using a physics-based modeling approach in
732 the Seine watershed (Schuite et al., 2019).

733

734 On the scale of the whole Metropolitan France area, however, due to the lack of data about physical
735 properties of aquifers and an insufficient gathering of existing data into a database, it would be hazardous
736 to get any further into the interpretation of the impact of physical properties on the significance of low-
737 frequency variabilities in groundwater levels. Hence, the development of such a database gathering the
738 physical properties of aquifers near boreholes across Metropolitan France would be useful for further
739 investigations.

740

741 4.3. Influence of multi-annual and decadal variabilities on groundwater trends and 742 comparison with their influence on (effective) precipitation trends

743 Our analyses emphasized the need for long groundwater time series to get better insight into the
744 existence and meaning of trends regarding the presence of low-frequency variability. Extending the
745 groundwater time series period by 20 years revealed a decrease in the influence of multi-annual
746 variability (~7-yr) on trends. Thus, this component only little affected the trend. Obviously, the
747 significance of this influence also depends on the water table behaviour and thus on the relative
748 importance of multi-annual or decadal variabilities in the total variance of groundwater levels. The more
749 the considered variability (multi-annual or decadal) dominates groundwater levels, the more influence
750 it has on the trend.

751

752 We also noted that some trends carried by either the multi-annual or decadal variability, are caused by
753 changes in the amplitude of the low-frequency variabilities over time. These regular changes in the
754 variance of low-frequency variabilities have been highlighted in many precipitation and streamflow
755 studies (Fritier et al., 2012; Dieppois et al., 2013 and 2016; Massei et al., 2010 and 2017). In the
756 Normandy chalk, downward trends detected in groundwater levels seem to be partly related to a
757 weakening of the low-frequency variability over time, the decadal variability appearing to be the main

758 responsible for these downward trends. Its removal largely influenced trends (they became much smaller
759 in magnitude), whereas that of multi-annual variability did little or not affect trend magnitude. This may
760 also explain the stable downward trends detected in Normandy chalk and why changing the time series
761 length has no effect on trend direction.

762

763 In Section 3.3., we demonstrated the significant influence of multi-annual and decadal variabilities on
764 groundwater level trends. This large influence of such low-frequency variabilities on groundwater trends
765 raises the following question: is this influence inherent to the aquifer systems, or does it influence trends
766 of precipitation and effective precipitation in the same way? We thus also analysed these variables to
767 answer this question.

768

769 In all hydrogeological units of the Paris Basin, the decadal variability drives groundwater levels down
770 and thus aggravates downward trends over the 1976–2019 period (Fig. 9). Our analyses on precipitation
771 and effective precipitation showed primarily the same influence of decadal variability on precipitation
772 and effective precipitation trends as on groundwater levels (Fig. 11). It drives precipitation levels down,
773 attenuating upward trends and accentuating downward trends. These consistent results indicate that this
774 influence of decadal variability on groundwater trends is climatologically induced and is not affected
775 by catchment and aquifer systems.

776

777 **Figure 11.** *Comparison of precipitation trend magnitude between cumulated monthly precipitation,*
778 *~7-yr filtered cumulated monthly precipitation and ~17-yr filtered cumulated monthly precipitation*
779 *over 1976–2019;*

780 *a) and b) show precipitation results, c) and d) show effective precipitation results.*

781 *The legend of hydrogeological entities can be found on Figure 8.*

782

783 Our study also revealed a reversal of the effect pattern of multi-annual variability on trends over the
784 1996–2019 period between aquifers in northern and southern France (Fig. 8). The analysis of
785 precipitation (P) data showed that over all of France the influence of multi-annual variability on trends

786 is homogeneous: it drives precipitation levels down, attenuating upward trends and accentuating
787 downward trends (Fig. 12). Thus, the influence of multi-annual variability on trends indicates a reversed
788 pattern between precipitation and groundwater levels in northern France, particularly in the Paris Basin.
789 Either potential evapotranspiration (PET) and/or aquifer properties may affect the influence of multi-
790 annual variability on trends and reverse its effect. However, we observed a similar influence of multi-
791 annual variability on effective precipitation (EP) trends as on groundwater trends in the Paris Basin,
792 driving effective precipitation levels up (Fig. 13). Knowing that EP is equivalent to P-PET, this result
793 suggests that PET would be responsible for this reversal pattern between precipitation and groundwater
794 levels, rather than catchment and aquifer properties.

795

796 *Figure 12. Comparison of precipitation trend magnitude between cumulated monthly precipitation*
797 *and ~7-yr filtered cumulated monthly precipitation over 1996–2019.*

798

799 *Figure 13. Comparison of effective precipitation trend magnitude between cumulated monthly*
800 *effective precipitation and ~7-yr filtered cumulated monthly effective precipitation over 1996–2019.*

801

802 In southern France, over the 1996–2019 period, the influence of multi-annual variability is the same on
803 precipitation trends, effective precipitation trends and groundwater trends (Fig. 8, 12 and 13). Only the
804 Mediterranean region shows atypical results, as the multi-annual variability drives precipitation and
805 groundwater levels down, while driving effective precipitation levels up. This indicates that, first, PET
806 would affect the influence of multi-annual variability on trends by reversing the effect between
807 precipitation and effective precipitation, and second, that catchments and aquifer properties would affect
808 this influence in turn to reverse it again between effective precipitation and groundwater levels. To better
809 understand and explain this phenomenon, further investigations will be necessary at a regional scale.

810

811 Over the longer period of 1976–2019, the influence of multi-annual variability on trends of precipitation,
812 effective precipitation and groundwater levels is heterogeneous in northern France (Fig. 9 and 11). Some
813 regions (Normandy, Champagne, and Artois-Picardy) show a rather consistent influence of multi-annual

814 variability on trends, regardless of the variable (precipitation, effective precipitation, groundwater
815 levels). For these regions, the multi-annual variability primarily drives levels up (attenuating downward
816 trends or accentuating upward trends). In other regions however, such as Bessin, Beauce and Bourgogne,
817 the available data indicate different influences of multi-annual variability on precipitation, effective
818 precipitation, and groundwater level trends. We will not extend the discussion to these regions because
819 the results showed disparities at the local scale.

820

821 Our analysis provides a first insight into the influence of multi-annual and decadal variabilities in
822 groundwater levels on estimated trends. Generally, the influence of both low-frequency variabilities is
823 also similar on precipitation and effective precipitation trends. We observe multi-annual and decadal
824 variabilities that aggravate downward trends or mitigate upward trends either in groundwater,
825 precipitation and effective precipitation. It is known that low-frequency variability (originating from
826 internal climate variability) may modulate anthropogenically-driven trends, particularly those induced
827 by climate change (Kingston et al., 2020). Our result indicates that low-frequency variabilities would be
828 able to aggravate trends (i.e., amplify downward trends) that might be induced by anthropogenic climate
829 change. For regions that are already submitted to regular meteorological and hydrological droughts, this
830 result may be particularly alarming, such as for the Mediterranean region that is defined as an
831 anthropogenic climate change “hotspot” (Diffenbaugh and Giorgi, 2012; Lionello and Scarascia, 2018;
832 Drobinski et al., 2020; Trambly et al., 2020). However, even if it is accepted that low-frequency
833 variability may accentuate, attenuate or inverse the long-term effects of climate change on hydrological
834 processes (Fatichi et al., 2014; Gu et al., 2019; Massei et al., 2020), our methodology in this article does
835 not allow us to obtain residual trends that may be only related to climate change. Indeed, we subtracted
836 individually each low-frequency variability to assess their specific influence on trends and consequently
837 there is still some low-frequency in residual time series (filtered ones) on which the trend is re-estimated.
838 Consequently, we do not estimate directly the aggravating or mitigating potential of low-frequency
839 variability on trends that would be related only to climate change.

840

841 In some areas, however, discrepancies exist between precipitation and effective precipitation, suggesting
842 the possible influence of PET that inverses the effect of multi-annual variability on trends (over 1996–
843 2019) in the Paris Basin. Locally, discrepancies can appear between effective precipitation and
844 groundwater levels, such as in the Beauce area over 1976–2019 due to aquifer properties that
845 significantly filter the multi-annual variability, which then no longer affects groundwater trends. Further
846 investigations will be necessary to better understand the processes and physical properties causing the
847 reversal of the influence of low-frequency variability on trends between precipitation and groundwater
848 levels.

849

850 The large influence of low-frequency variability on estimated groundwater level trends entails several
851 implications. First regarding conclusions about traces of climate change in groundwater levels, since
852 trends may actually correspond to the presence of low-frequency variability, and then be primarily the
853 result of internal climate variability instead of anthropogenic climate change. Second regarding future
854 evolutions of groundwater levels, since a potential change in the amplitude of internal climate variability
855 (that may also be the consequence of anthropogenic climate change) – e.g. increasing or decreasing low-
856 frequency variability – in the next decades may lead to substantial changes in groundwater level trends.
857 Consequently, the extrapolation of trends estimated over the historical period seems particularly
858 hazardous, due to the stochastic and unpredictable behaviour of such low-frequency fluctuations. Third
859 regarding future projections, because internal climate variability is often improperly reproduced and is
860 a major source of uncertainties in climate and hydrological projections resulting from GCM outputs
861 (Terray and Boé, 2013; Qasmi et al., 2017). Consequently, trend estimates resulting from these
862 hydrological projections (and *in fine* resulting from recharge and groundwater level projections) would
863 be subject to strong uncertainty.

864

865 **5. Conclusion**

866 The analysis of groundwater level trends in France showed that a number of aquifers were susceptible
867 to trend direction instabilities (i.e., changes in trend direction according to the length of time series),

868 leading to contradictory conclusions about groundwater level evolutions. This led to the question of the
869 existence, importance and spatial distribution of low-frequency variability in groundwater levels of
870 French aquifers. Groundwater levels were therefore broken down by MODWT to estimate the
871 significance of low-frequency variabilities in total groundwater level variability. It turned out that most
872 of aquifers susceptible to trend direction instabilities exhibit a hydrological variability characterized by
873 a significant low-frequency variability: they are aquifers with inertial or combined behaviour of water
874 tables. Given the significant presence of multi-annual and decadal variabilities in groundwater levels,
875 we aimed to determine if, how and to what extent each of these components could affect trend estimates.
876 To this end, MODWT filtering was performed to subtract individually the multi-annual or decadal
877 variability from the entire signal, and then trends were re-estimated on the filtered groundwater level
878 time series. The results showed that the groundwater level trends were highly sensitive to the presence
879 of any of these low-frequency components, which may then strongly influence the estimated trends.
880 Such results indicate that low-frequency variability (originating from internal climate variability) is
881 capable of attenuating or accentuating groundwater level trends, including those that might be associated
882 with climate change.

883

884 In general, trend detection is widely used as a tool for assessing changes in groundwater levels.
885 Nevertheless, our study presents features that show that this tool should be used with caution,
886 particularly for studying groundwater levels with significant low-frequency variability. We observed
887 that: (i) trends are highly dependent upon the study period and time series length, and cannot be
888 extrapolated; (ii) trends are strongly influenced and guided by low-frequency variability, and (iii) trends
889 are often only segments of larger scale fluctuations resulting from large-scale atmospheric or oceanic
890 circulation. Consequently, their interpretation and attribution to a physical phenomenon, such as climate
891 change *vs.* climate variability, remains complex. In addition, since low-frequency variability strongly
892 guides and influences the estimated groundwater level trends, potential changes in low-frequency
893 variability – induced by changes in internal climate variability – would necessarily lead to a change in
894 the estimated trends. In particular, this means that (i) estimation of trends in hydrological projections
895 resulting from GCM outputs in which low-frequency variability is not well represented would be

896 subject to strong uncertainty, (ii) a potential change in internal climate variability – e.g. increasing or
897 decreasing low-frequency variability – in the next decades may lead to substantial changes in estimated
898 groundwater level trends.

899

900 Consequently, future works should focus on assessing the impacts of a potential change in internal
901 climate variability (i.e., low-frequency variability) on groundwater level trends using different scenarios
902 of amplitude-modifications of low-frequency variability. In addition, a sensitivity analysis of the results
903 of this study to decomposition method employed (e.g. wavelets, EEMD) should be conducted.

904

905 **Acknowledgments**

906

907 This work was partially supported by the GeoERA project TACTIC, funded by the European Union's
908 Horizon 2020 research and innovation programme under grant agreement number 731166. We would
909 also like to thank the AESN and PIREN Seine programs for their support. Finally, we would like to
910 thank Sandra Lanini for the calculation of effective precipitation; the two anonymous reviewers for their
911 thoughtful comments that definitely helped improving the paper; Marinus Kluijver for editing the final
912 English version; Jean-Jacques Seguin, Marc Laurencelle and Laurence Gourcy for the helpful
913 discussions.

914

915 **References**

916 Baulon, L., Allier, D., Massei, N., Bessiere, H., Fournier, M., Bault, V., 2020. Influence de la
917 variabilité basse-fréquence des niveaux piézométriques sur l'occurrence et l'amplitude des
918 extrêmes. *Géologues* 207, 53–60.

919 Blöschl, G., Hall, J., Viglione, A., Perdigão, R.A.P., Parajka, J., Merz, B., Lun, D., Arheimer, B.,
920 Aronica, G.T., Bilibashi, A., Boháč, M., Bonacci, O., Borga, M., Čanjevac, I., Castellarin, A.,
921 Chirico, G.B., Claps, P., Frolova, N., Ganora, D., Gorbachova, L., Gül, A., Hannaford, J.,

922 Harrigan, S., Kireeva, M., Kiss, A., Kjeldsen, T.R., Kohnová, S., Koskela, J.J., Ledvinka, O.,
923 Macdonald, N., Mavrova-Guirguinova, M., Mediero, L., Merz, R., Molnar, P., Montanari, A.,
924 Murphy, C., Osuch, M., Ovcharuk, V., Radevski, I., Salinas, J.L., Sauquet, E., Šraj, M.,
925 Szolgay, J., Volpi, E., Wilson, D., Zaimi, K., Živković, N., 2019. Changing climate both
926 increases and decreases European river floods. *Nature* 573, 108–111.
927 <https://doi.org/10.1038/s41586-019-1495-6>

928 Boé, J., Habets, F., 2014. Multi-decadal river flow variations in France. *Hydrology and Earth System*
929 *Sciences* 18, 691–708. <https://doi.org/10.5194/hess-18-691-2014>

930 Burn, D.H., Hannaford, J., Hodgkins, G.A., Whitfield, P.H., Thorne, R., Marsh, T., 2012. Reference
931 hydrologic networks II. Using reference hydrologic networks to assess climate-driven changes
932 in streamflow. *Hydrological Sciences Journal* 57, 1580–1593.
933 <https://doi.org/10.1080/02626667.2012.728705>

934 Burn, D.H., Whitfield, P.H., 2018. Changes in flood events inferred from centennial length streamflow
935 data records. *Advances in Water Resources* 121, 333–349.
936 <https://doi.org/10.1016/j.advwatres.2018.08.017>

937 Caesar, L., Rahmstorf, S., Robinson, A., Feulner, G., Saba, V., 2018. Observed fingerprint of a
938 weakening Atlantic Ocean overturning circulation. *Nature* 556, 191–196.
939 <https://doi.org/10.1038/s41586-018-0006-5>

940 Caporali, E., Lompi, M., Pacetti, T., Chiarello, V., Fatichi, S., 2020. A review of studies on observed
941 precipitation trends in Italy. *International Journal of Climatology* 41, 1–25.
942 <https://doi.org/10.1002/joc.6741>

943 Chataigner, J., Michon, J., 2019. Prélèvements quantitatifs sur la ressource en eau (données 2016).
944 Agence française pour la biodiversité (AFB), 12pp.

945 Constantine, W., Percival, D., 2016. wmtsa: Wavelet Methods for Time Series Analysis. R package
946 version 2.0-1. <<https://CRAN.R-project.org/package=wmtsa>>.

947 Cornish, C.R., Bretherton, C.S., Percival, D.B., 2006. Maximal Overlap Wavelet Statistical Analysis
948 With Application to Atmospheric Turbulence. *Boundary-Layer Meteorol* 119, 339–374.
949 <https://doi.org/10.1007/s10546-005-9011-y>

950 Cornish, C. R., Percival, D. B., Bretherton, C. S., 2003. The WMTSA Wavelet Toolkit for Data
951 Analysis in the Geosciences. *EOS Trans AGU*. 84(46): Fall Meet. Suppl., Abstract NG11A-
952 0173

953 Degefu, M.A., Alamirew, T., Zeleke, G., Bewket, W., 2019. Detection of trends in hydrological
954 extremes for Ethiopian watersheds, 1975–2010. *Reg Environ Change* 19, 1923–1933.
955 <https://doi.org/10.1007/s10113-019-01510-x>

956 Dieppois, B., Durand, A., Fournier, M., Massei, N., 2013. Links between multidecadal and
957 interdecadal climatic oscillations in the North Atlantic and regional climate variability of
958 northern France and England since the 17th century. *Journal of Geophysical Research:*
959 *Atmospheres* 118, 4359–4372. <https://doi.org/10.1002/jgrd.50392>

960 Dieppois, B., Lawler, D.M., Slonosky, V., Massei, N., Bigot, S., Fournier, M., Durand, A., 2016.
961 Multidecadal climate variability over northern France during the past 500 years and its
962 relation to large-scale atmospheric circulation. *International Journal of Climatology* 36, 4679–
963 4696. <https://doi.org/10.1002/joc.4660>

964 Diffenbaugh, N.S., Giorgi, F., 2012. Climate change hotspots in the CMIP5 global climate model
965 ensemble. *Climatic Change* 114, 813–822. <https://doi.org/10.1007/s10584-012-0570-x>

966 Dong, B., Sutton, R.T., Woollings, T., 2011. Changes of interannual NAO variability in response to
967 greenhouse gases forcing. *Clim Dyn* 37, 1621–1641. <https://doi.org/10.1007/s00382-010->
968 0936-6

969 Drobinski, P., Da Silva, N., Bastin, S., Mailler, S., Muller, C., Ahrens, B., Christensen, O.B., Lionello,
970 P., 2020. How warmer and drier will the Mediterranean region be at the end of the twenty-first
971 century? *Reg Environ Change* 20, 78. <https://doi.org/10.1007/s10113-020-01659-w>

972 Dudley, R.W., Hirsch, R.M., Archfield, S.A., Blum, A.G., Renard, B., 2020. Low streamflow trends at
973 human-impacted and reference basins in the United States. *Journal of Hydrology* 580, 124254.
974 <https://doi.org/10.1016/j.jhydrol.2019.124254>

975 Edijatno, Michel, C., 1989. Un modèle pluie-débit journalier à trois paramètres. *La Houille Blanche* 2,
976 113-122. <https://doi.org/10.1051/lhb/1989007>

977 El Janyani, S., Massei, N., Dupont, J.-P., Fournier, M., Dörfliger, N., 2012. Hydrological responses of
978 the chalk aquifer to the regional climatic signal. *Journal of Hydrology* 464–465, 485–493.
979 <https://doi.org/10.1016/j.jhydrol.2012.07.040>

980 Enfield, D.B., Mestas-Núñez, A.M., Trimble, P.J., 2001. The Atlantic Multidecadal Oscillation and its
981 relation to rainfall and river flows in the continental U.S. *Geophysical Research Letters* 28,
982 2077–2080. <https://doi.org/10.1029/2000GL012745>

983 Espinosa, L.A., Portela, M.M., 2020. Rainfall Trends over a Small Island Teleconnected to the North
984 Atlantic Oscillation - the Case of Madeira Island, Portugal. *Water Resour Manage.*
985 <https://doi.org/10.1007/s11269-020-02668-4>

986 European Commission, 2009. COMMON IMPLEMENTATION STRATEGY FOR THE WATER
987 FRAMEWORK DIRECTIVE (2000/60/EC) - Guidance Document n°18 - GUIDANCE ON
988 GROUNDWATER STATUS AND TREND ASSESSMENT – EC 2009, ISBN 978-92-79-
989 11374-1 - Chap. 5.3.1.

990 Fatichi, S., Rimkus, S., Burlando, P., Bordoy, R., 2014. Does internal climate variability overwhelm
991 climate change signals in streamflow? The upper Po and Rhone basin case studies. *Science of
992 The Total Environment* 493, 1171–1182. <https://doi.org/10.1016/j.scitotenv.2013.12.014>

993 Fatichi, S., Molnar, P., Mastrotheodoros, T., Burlando, P., 2015a. Diurnal and seasonal changes in
994 near-surface humidity in a complex orography. *Journal of Geophysical Research:
995 Atmospheres* 120, 2358–2374. <https://doi.org/10.1002/2014JD022537>

996 Fossa, M., Dieppois, B., Massei, N., Fournier, M., Laignel, B., Vidal, J.-P., 2021. Spatio-temporal and
997 cross-scale interactions in hydroclimate variability: a case-study in France. *Hydrology and
998 Earth System Sciences Discussions* 1–29. <https://doi.org/10.5194/hess-2021-81>

999 Fritier, N., Massei, N., Laignel, B., Durand, A., Dieppois, B., Deloffre, J., 2012. Links between NAO
1000 fluctuations and inter-annual variability of winter-months precipitation in the Seine River
1001 watershed (north-western France). *Comptes Rendus Geoscience* 344, 396–405.
1002 <https://doi.org/10.1016/j.crte.2012.07.004>

1003 Giuntoli, I., Renard, B., Vidal, J.-P., Bard, A., 2013. Low flows in France and their relationship to
1004 large-scale climate indices. *Journal of Hydrology* 482, 105–118.
1005 <https://doi.org/10.1016/j.jhydrol.2012.12.038>

1006 Gouhier, T.C., Grinsted, A., 2012. biwavelet: Conduct univariate and bivariate wavelet analyses. R
1007 package version 0.12. <<http://CRAN.R-project.org/package=biwavelet>>.

1008 Gu, L., Chen, J., Xu, C.-Y., Kim, J.-S., Chen, H., Xia, J., Zhang, L., 2019. The contribution of internal
1009 climate variability to climate change impacts on droughts. *Science of The Total Environment*
1010 684, 229–246. <https://doi.org/10.1016/j.scitotenv.2019.05.345>

1011 Gudmundsson, L., Tallaksen, L.M., Stahl, K., Fleig, A.K., 2011. Low-frequency variability of
1012 European runoff. *Hydrol. Earth Syst. Sci.* 15, 2853–2869. [https://doi.org/10.5194/hess-15-](https://doi.org/10.5194/hess-15-2853-2011)
1013 [2853-2011](https://doi.org/10.5194/hess-15-2853-2011)

1014 Guo, B., Chen, Z., Guo, J., Liu, F., Chen, C., Liu, K., 2016. Analysis of the Nonlinear Trends and
1015 Non-Stationary Oscillations of Regional Precipitation in Xinjiang, Northwestern China, Using
1016 Ensemble Empirical Mode Decomposition. *International Journal of Environmental Research
1017 and Public Health* 13, 345. <https://doi.org/10.3390/ijerph13030345>

1018 Hamed, K.H., Ramachandra Rao, A., 1998. A modified Mann-Kendall trend test for autocorrelated
1019 data. *Journal of Hydrology* 204, 182–196. [https://doi.org/10.1016/S0022-1694\(97\)00125-X](https://doi.org/10.1016/S0022-1694(97)00125-X)

1020 Hannaford, J., Buys, G., Stahl, K., Tallaksen, L.M., 2013. The influence of decadal-scale variability
1021 on trends in long European streamflow records. *Hydrology and Earth System Sciences* 17,
1022 2717–2733. <https://doi.org/10.5194/hess-17-2717-2013>

1023 Iliopoulou, T., Koutsoyiannis, D., 2020. Projecting the future of rainfall extremes: Better classic than
1024 trendy. *Journal of Hydrology* 588, 125005. <https://doi.org/10.1016/j.jhydrol.2020.125005>

1025 Kendall, M.G., Stuart, A., Ord, J.K., 1987. Kendall’s advanced theory of statistics. Oxford University
1026 Press, Inc., USA.

1027 Kerr, R.A., 2000. A North Atlantic Climate Pacemaker for the Centuries. *Science* 288, 1984–1985.
1028 <https://doi.org/10.1126/science.288.5473.1984>

1029 Kingston, D.G., Massei, N., Dieppois, B., Hannah, D.M., Hartmann, A., Lavers, D.A., Vidal, J.-P.,
1030 2020. Moving beyond the catchment scale: Value and opportunities in large-scale hydrology

1031 to understand our changing world. *Hydrological Processes* 34, 2292–2298.
1032 <https://doi.org/10.1002/hyp.13729>

1033 Koutsoyiannis, D., 2006. Nonstationarity versus scaling in hydrology. *Journal of Hydrology* 324, 239–
1034 254. <https://doi.org/10.1016/j.jhydrol.2005.09.022>

1035 Liesch, T., Wunsch, A., 2019. Aquifer responses to long-term climatic periodicities. *Journal of*
1036 *Hydrology* 572, 226–242. <https://doi.org/10.1016/j.jhydrol.2019.02.060>

1037 Lionello, P., Scarascia, L., 2018. The relation between climate change in the Mediterranean region and
1038 global warming. *Reg Environ Change* 18, 1481–1493. [https://doi.org/10.1007/s10113-018-](https://doi.org/10.1007/s10113-018-1290-1)
1039 1290-1

1040 Lorenzo-Lacruz, J., Vicente-Serrano, S.M., López-Moreno, J.I., Morán-Tejeda, E., Zabalza, J., 2012.
1041 Recent trends in Iberian streamflows (1945–2005). *Journal of Hydrology* 414–415, 463–475.
1042 <https://doi.org/10.1016/j.jhydrol.2011.11.023>

1043 McCabe, G.J., Wolock, D.M., 2002. A step increase in streamflow in the conterminous United States.
1044 *Geophysical Research Letters* 29, 38-1-38-4. <https://doi.org/10.1029/2002GL015999>

1045 Mann, H.B., 1945. Nonparametric Tests Against Trend. *Econometrica* 13, 245–259.
1046 <https://doi.org/10.2307/1907187>

1047 Massei, N., Dieppois, B., Hannah, D.M., Lavers, D.A., Fossa, M., Laignel, B., Debret, M., 2017.
1048 Multi-time-scale hydroclimate dynamics of a regional watershed and links to large-scale
1049 atmospheric circulation: Application to the Seine river catchment, France. *Journal of*
1050 *Hydrology* 546, 262–275. <https://doi.org/10.1016/j.jhydrol.2017.01.008>

1051 Massei, N., Durand, A., Deloffre, J., Dupont, J.P., Valdes, D., Laignel, B., 2007. Investigating
1052 possible links between the North Atlantic Oscillation and rainfall variability in northwestern
1053 France over the past 35 years. *Journal of Geophysical Research: Atmospheres* 112.
1054 <https://doi.org/10.1029/2005JD007000>

1055 Massei, N., Fournier, M., 2012. Assessing the expression of large-scale climatic fluctuations in the
1056 hydrological variability of daily Seine river flow (France) between 1950 and 2008 using
1057 Hilbert–Huang Transform. *Journal of Hydrology* 448–449, 119–128.
1058 <https://doi.org/10.1016/j.jhydrol.2012.04.052>

1059 Massei, N., Kingston, D.G., Hannah, D.M., Vidal, J.-P., Dieppo, B., Fossa, M., Hartmann, A.,
1060 Lavers, D.A., Laignel, B., 2020. Understanding and predicting large-scale hydrological
1061 variability in a changing environment, in: Proceedings of the International Association of
1062 Hydrological Sciences. Presented at the Hydrological processes and water security in a
1063 changing world - Hydrological Processes and Water Security in a Changing World, Beijing,
1064 China, 6–9 November 2018, Copernicus GmbH, pp. 141–149. [https://doi.org/10.5194/piahs-](https://doi.org/10.5194/piahs-383-141-2020)
1065 [383-141-2020](https://doi.org/10.5194/piahs-383-141-2020)

1066 Massei, N., Laignel, B., Deloffre, J., Mesquita, J., Motelay, A., Lafite, R., Durand, A., 2010. Long-
1067 term hydrological changes of the Seine River flow (France) and their relation to the North
1068 Atlantic Oscillation over the period 1950–2008. *International Journal of Climatology* 30,
1069 2146–2154. <https://doi.org/10.1002/joc.2022>

1070 Mohanavelu, A., Kasiviswanathan, K.S., Mohanasundaram, S., Ilampooranan, I., He, J., Pingale, S.M.,
1071 Soundharajan, B.-S., Diwan Mohaideen, M.M., 2020. Trends and Non-Stationarity in
1072 Groundwater Level Changes in Rapidly Developing Indian Cities. *Water* 12, 3209.
1073 <https://doi.org/10.3390/w12113209>

1074 Morin, E., 2011. To know what we cannot know: Global mapping of minimal detectable absolute
1075 trends in annual precipitation. *Water Resources Research* 47.
1076 <https://doi.org/10.1029/2010WR009798>

1077 Neves, M.C., Jerez, S., Trigo, R.M., 2019. The response of piezometric levels in Portugal to NAO,
1078 EA, and SCAND climate patterns. *Journal of Hydrology* 568, 1105–1117.
1079 <https://doi.org/10.1016/j.jhydrol.2018.11.054>

1080 Pathak, A.A., Dodamani, B.M., 2019. Trend Analysis of Groundwater Levels and Assessment of
1081 Regional Groundwater Drought: Ghataprabha River Basin, India. *Nat Resour Res* 28, 631–
1082 643. <https://doi.org/10.1007/s11053-018-9417-0>

1083 Peña-Angulo, D., Vicente-Serrano, S.M., Domínguez-Castro, F., Murphy, C., Reig, F., Trambly, Y.,
1084 Trigo, R.M., Luna, M.Y., Turco, M., Noguera, I., Aznárez-Balta, M., García-Herrera, R.,
1085 Tomas-Burguera, M., Kenawy, A.E., 2020. Long-term precipitation in Southwestern Europe

1086 reveals no clear trend attributable to anthropogenic forcing. *Environ. Res. Lett.* 15, 094070.
1087 <https://doi.org/10.1088/1748-9326/ab9c4f>

1088 Percival, D.B., Mofjeld, H.O., 1997. Analysis of Subtidal Coastal Sea Level Fluctuations Using
1089 Wavelets. *Journal of the American Statistical Association* 92, 868–880.
1090 <https://doi.org/10.1080/01621459.1997.10474042>

1091 Percival, D. B., Walden, A. T., 2000. *Wavelet Methods for Time Series Analysis*. Cambridge
1092 University Press, Cambridge.

1093 Pérez Ciria, T., Labat, D., Chiogna, G., 2019. Detection and interpretation of recent and historical
1094 streamflow alterations caused by river damming and hydropower production in the Adige and
1095 Inn river basins using continuous, discrete and multiresolution wavelet analysis. *Journal of*
1096 *Hydrology* 578, 124021. <https://doi.org/10.1016/j.jhydrol.2019.124021>

1097 Qasmi, S., Cassou, C., Boé, J., 2017. Teleconnection Between Atlantic Multidecadal Variability and
1098 European Temperature: Diversity and Evaluation of the Coupled Model Intercomparison
1099 Project Phase 5 Models. *Geophysical Research Letters* 44, 11,140–11,149.
1100 <https://doi.org/10.1002/2017GL074886>

1101 Rossi, A., Massei, N., Laignel, B., 2011. A synthesis of the time-scale variability of commonly used
1102 climate indices using continuous wavelet transform. *Global and Planetary Change* 78, 1–13.
1103 <https://doi.org/10.1016/j.gloplacha.2011.04.008>

1104 Roux, J.C., 2006. *Aquifères et eaux souterraines en France*. BRGM Editions, 956p.

1105 Rust, W., Holman, I., Bloomfield, J., Cuthbert, M., Corstanje, R., 2019. Understanding the potential of
1106 climate teleconnections to project future groundwater drought. [https://doi.org/10.5194/hess-](https://doi.org/10.5194/hess-23-3233-2019)
1107 [23-3233-2019](https://doi.org/10.5194/hess-23-3233-2019)

1108 Rust, W., Holman, I., Corstanje, R., Bloomfield, J., Cuthbert, M., 2018. A conceptual model for
1109 climatic teleconnection signal control on groundwater variability in Europe. *Earth-Science*
1110 *Reviews* 177, 164–174. <https://doi.org/10.1016/j.earscirev.2017.09.017>

1111 Sakizadeh, M., Mohamed, M.M.A., Klammler, H., 2019. Trend Analysis and Spatial Prediction of
1112 Groundwater Levels Using Time Series Forecasting and a Novel Spatio-Temporal Method.
1113 *Water Resour Manage* 33, 1425–1437. <https://doi.org/10.1007/s11269-019-02208-9>

1114 Sang, Y.-F., Wang, Z., Liu, C., 2014. Comparison of the MK test and EMD method for trend
1115 identification in hydrological time series. *Journal of Hydrology* 510, 293–298.
1116 <https://doi.org/10.1016/j.jhydrol.2013.12.039>

1117 Schmockler-Fackel, P., Naef, F., 2010. More frequent flooding? Changes in flood frequency in
1118 Switzerland since 1850. *Journal of Hydrology* 381, 1–8.
1119 <https://doi.org/10.1016/j.jhydrol.2009.09.022>

1120 Schuite, J., Flipo, N., Massei, N., Rivière, A., Baratelli, F., 2019. Improving the Spectral Analysis of
1121 Hydrological Signals to Efficiently Constrain Watershed Properties. *Water Resources*
1122 *Research* 55, 4043–4065. <https://doi.org/10.1029/2018WR024579>

1123 Sen, P.K., 1968. Estimates of the Regression Coefficient Based on Kendall's Tau. *Biometrika* 63, 1379–1389.
1124 <https://doi.org/10.1080/01621459.1968.10480934>

1125 Slimani, S., Massei, N., Mesquita, J., Valdés, D., Fournier, M., Laignel, B., Dupont, J.-P., 2009.
1126 Combined climatic and geological forcings on the spatio-temporal variability of piezometric
1127 levels in the chalk aquifer of Upper Normandy (France) at pluridecennial scale. *Hydrogeol J*
1128 17, 1823. <https://doi.org/10.1007/s10040-009-0488-1>

1129 Song, X., Song, Y., Chen, Y., 2020. Secular trend of global drought since 1950. *Environ. Res. Lett.*
1130 15, 094073. <https://doi.org/10.1088/1748-9326/aba20d>

1131 Stahl, K., Hisdal, H., Hannaford, J., Tallaksen, L., Van Lanen, H., Sauquet, E., Demuth, S.,
1132 Fendekova, M., Jordar, J., 2010. Streamflow trends in Europe: evidence from a dataset of
1133 near-natural catchments. *Hydrology and Earth System Sciences* 14, 2367–2382.
1134 <https://doi.org/10.5194/hess-14-2367-2010>

1135 Stojković, M., Ilić, A., Prohaska, S., Plavšić, J., 2014. Multi-Temporal Analysis of Mean Annual and
1136 Seasonal Stream Flow Trends, Including Periodicity and Multiple Non-Linear Regression.
1137 *Water Resour Manage* 28, 4319–4335. <https://doi.org/10.1007/s11269-014-0753-5>

1138 Tegel, W., Seim, A., Skiadaresis, G., Ljungqvist, F.C., Kahle, H.-P., Land, A., Muigg, B., Nicolussi,
1139 K., Büntgen, U., 2020. Higher groundwater levels in western Europe characterize warm
1140 periods in the Common Era. *Scientific Reports* 10, 16284. [https://doi.org/10.1038/s41598-](https://doi.org/10.1038/s41598-020-73383-8)
1141 [020-73383-8](https://doi.org/10.1038/s41598-020-73383-8)

1142 Terray, L., Boé, J., 2013. Quantifying 21st-century France climate change and related uncertainties.
1143 *Comptes Rendus Geoscience* 345, 136–149. <https://doi.org/10.1016/j.crte.2013.02.003>

1144 Torrence, C., Compo, G.P., 1998. A Practical Guide to Wavelet Analysis. *Bulletin of the American*
1145 *Meteorological Society* 79, 61–78.
1146 [https://doi.org/10.1175/1520-0477\(1998\)079<0061:APGTWA>2.0.CO;2](https://doi.org/10.1175/1520-0477(1998)079<0061:APGTWA>2.0.CO;2)

1147 Tramblay, Y., Koutroulis, A., Samaniego, L., Vicente-Serrano, S.M., Volaire, F., Boone, A., Le Page,
1148 M., Llasat, M.C., Albergel, C., Burak, S., Cailleret, M., Kalin, K.C., Davi, H., Dupuy, J.-L.,
1149 Greve, P., Grillakis, M., Hanich, L., Jarlan, L., Martin-StPaul, N., Martínez-Vilalta, J.,
1150 Mouillot, F., Pulido-Velazquez, D., Quintana-Seguí, P., Renard, D., Turco, M., Türkeş, M.,
1151 Trigo, R., Vidal, J.-P., Vilagrosa, A., Zribi, M., Polcher, J., 2020. Challenges for drought
1152 assessment in the Mediterranean region under future climate scenarios. *Earth-Science*
1153 *Reviews* 210, 103348. <https://doi.org/10.1016/j.earscirev.2020.103348>

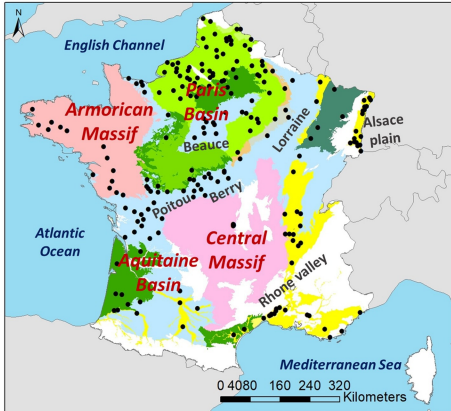
1154 Velasco, E.M., Gurdak, J.J., Dickinson, J.E., Ferré, T.P.A., Corona, C.R., 2017. Interannual to
1155 multidecadal climate forcings on groundwater resources of the U.S. West Coast. *Journal of*
1156 *Hydrology: Regional Studies, Water, energy, and food nexus in the Asia-Pacific region* 11,
1157 250–265. <https://doi.org/10.1016/j.ejrh.2015.11.018>

1158 Vicente-Serrano, S.M., Peña-Gallardo, M., Hannaford, J., Murphy, C., Lorenzo-Lacruz, J.,
1159 Dominguez-Castro, F., López-Moreno, J.I., Beguería, S., Noguera, I., Harrigan, S., Vidal, J.-
1160 P., 2019. Climate, Irrigation, and Land Cover Change Explain Streamflow Trends in
1161 Countries Bordering the Northeast Atlantic. *Geophysical Research Letters* 46, 10821–10833.
1162 <https://doi.org/10.1029/2019GL084084>

1163 Vidal, J.-P., Martin, E., Franchistéguy, L., Baillon, M., Soubeyroux, J.-M., 2010. A 50-year high-
1164 resolution atmospheric reanalysis over France with the Safran system. *International Journal of*
1165 *Climatology* 30, 1627–1644. <https://doi.org/10.1002/joc.2003>

1166 Visser, A., Dubus, I., Broers, H.P., Brouyère, S., Korcz, M., Orban, P., Goderniaux, P., Batlle-Aguilar,
1167 J., Surdyk, N., Amraoui, N., Job, H., Pinault, J.L., Bierkens, M., 2009. Comparison of

1168 methods for the detection and extrapolation of trends in groundwater quality. *J. Environ.*
1169 *Monit.* 11, 2030–2043. <https://doi.org/10.1039/B905926A>
1170 Vu, M.T., Jardani, A., Massei, N., Fournier, M., 2020. Reconstruction of missing groundwater level
1171 data by using Long Short-Term Memory (LSTM) deep neural network. *Journal of Hydrology*
1172 125776. <https://doi.org/10.1016/j.jhydrol.2020.125776>



Legend

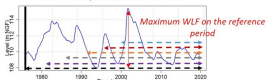
- Groundwater level observation wells

Aquifer group

- Bedrock
- Chalk
- Greensands
- Limestones
- Not studied formations
- Sand
- Sandstones
- Volcanic formations
- Alluvial formations

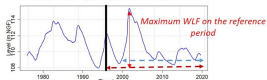
(a)**Step 1 : a. Assessment of Sen's slope; b. Normalisation by maximum WLF; c. Assignment to a magnitude class**

Reference period : 1976-2019



Well		1976-2019	1981-2019	1986-2019	1991-2019	1996-2019	2000-2019
Xn	Sen's slope						
	Sen/WLF						
	Class						

Reference period : 1996-2019



Well		1996-2019	2000-2019
Xn	Sen's slope		
	Sen/WLF		
	Class		

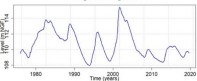
Step 2 : Class comparison

Well		1976-2019	1981-2019	1986-2019	1991-2019	1996-2019	2000-2019	Sign stability	Class stability
Xn	Class	Strong ↘	Strong ↘	Strong ↘	Moderate ↘	Strong ↘	Strong ↘	Still ↘	Unstable

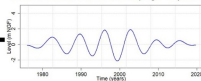
Well		1996-2019	2000-2019	Sign stability	Class stability
Xn	Class	Strong ↘	Strong ↘	Still ↘	Stable

(b)**Step 1 : Subtraction of the time scale of interest**

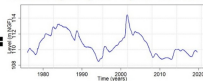
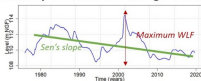
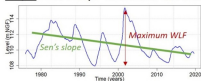
Original signal

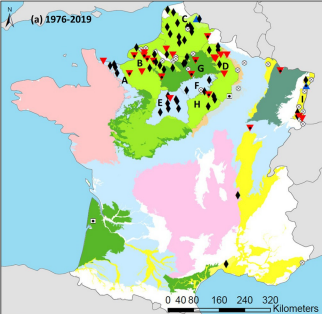


Wavelet detail subtracted (e.g. ~7 years)



Filtered signal of the ~7 years time scale

**Step 2 : Sen's slope calculation and normalisation by maximum WLF of original data**

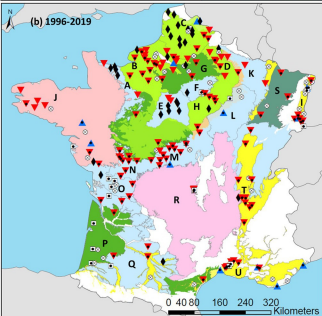


Legend

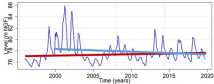
- Trend magnitude stability** Aquifer group
- Stable trend class
- Trend direction stability**
- ▲ Still upward trend
 - Still insignificant trend
 - ▼ Still downward trend
 - ◆ Change of sign
 - Emerging trend
- Aquifer group**
- Alluvial formations
 - Bedrock
 - Chalk
 - Greensands
 - Limestones
 - Sand
 - Sandstones
 - Volcanic formations
 - Not studied formations

Hydrogeological entities

- A Jurassic limestones from Sarthe to Bessin
- B Seno-Turonian chalk of Normandy/Picardy
- C Seno-Turonian chalk of Artois-Picardy
- D Seno-Turonian chalk of Champagne
- E Limestones of Beauce
- F Upper Eocene limestone of Paris Basin
- G Lutetian and Ypresian sands of Paris Basin
- H Upper Cretaceous chalk of Bourgogne
- I Alluvial formations of Alsace
- J Bedrock of Brittany
- K Jurassic limestones of Lorraine
- L Jurassic limestones of Côte-des-Bars
- M Jurassic limestones of Berry
- N Jurassic limestones of Poitou
- O Fractured Jurassic limestones of northern Aquitaine Basin
- P Plio-Quaternary sands of Aquitaine Basin
- Q Various calcareous formations of Aquitaine Basin
- R Volcanic formations of Central Massif
- S Triassic sandstones and limestones of Lorraine
- T Fluvio-glacial formations of Rhone valley
- U Alluvial formations of Mediterranean region



Beauval



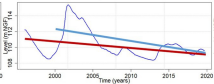
1996-2019 :

- Sen's slope = 0.2 cm/month
- Slope/WLF = 10% of WLF

2000-2019 :

- Sen's slope = -0.3 cm/month
- Slope/WLF = -13% of WLF

Goupillieres



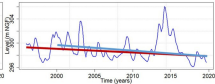
1996-2019 :

- Sen's slope = -0.7 cm/month
- Slope/WLF = -43% of WLF

2000-2019 :

- Sen's slope = -1.5 cm/month
- Slope/WLF = -76% of WLF

Penol

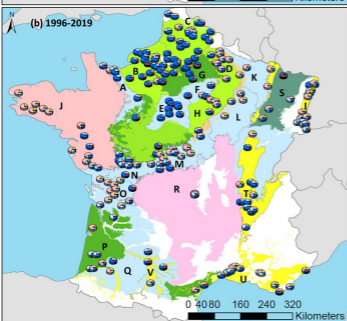
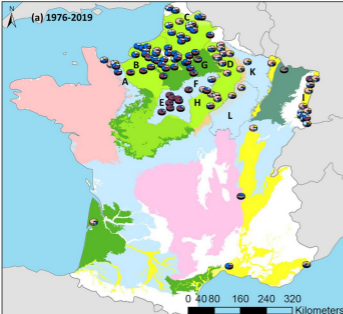


1996-2019 :

- Sen's slope = -0.4 cm/month
- Slope/WLF = -15% of WLF

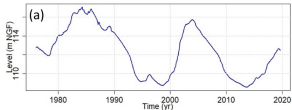
2000-2019 :

- Sen's slope = -0.6 cm/month
- Slope/WLF = -19% of WLF

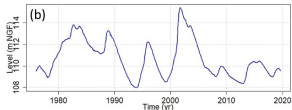


Limestones of Beauce

Inertial

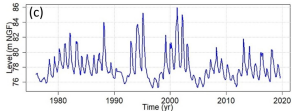


Seno-Turonian chalk of Normandy

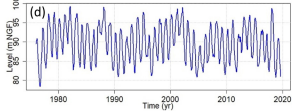


Seno-Turonian chalk of Artois-Picardy

Combined

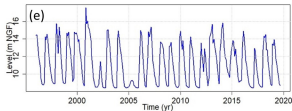


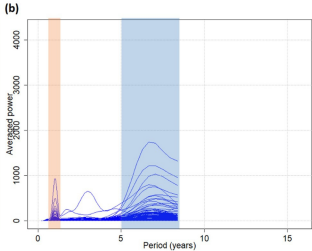
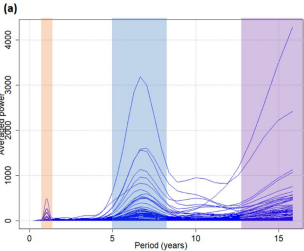
Seno-Turonian chalk of Champagne



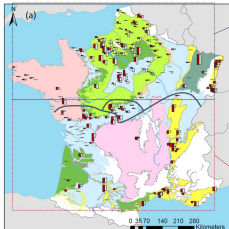
Jurassic limestones of northern Aquitaine Basin

Annual

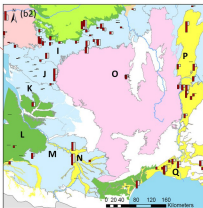
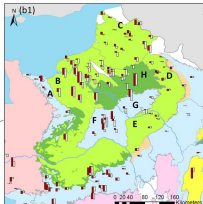




↗ ~7 years timescale drives upward groundwater levels



↘ ~7 years timescale drives downward groundwater levels



Ratio Sen's slope/maximum WLF



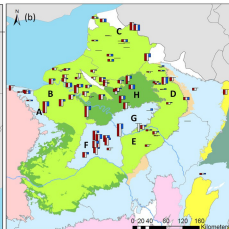
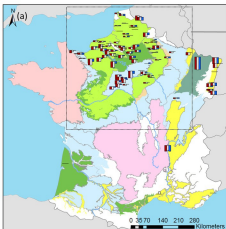
- Raw groundwater levels (monthly averages)
- 7yrs filtered groundwater levels
- ~ Pattern reversal boundary

Aquifer group

- Bedrock
- Chalk
- Greensands
- Limestones
- Not studied formations
- Sand
- Sandstones
- Volcanic formations
- Alluvial formations

Hydrogeological entities

- A Jurassic limestones from Sarthe to Bessin
- B Seno-Turonian chalk of Normandy/Picardy
- C Seno-Turonian chalk of Artois-Picardy Basin
- D Chalk of Champagne
- E Upper Cretaceous chalk of Bourgogne
- F Limestones of Beauce
- G Eocene limestones of Paris Basin
- H Lutetian and Ypresian sands of Paris Basin
- I Jurassic limestones of Poitou
- J Fractured Jurassic limestones of northern Aquitaine Basin
- K Upper Cretaceous limestones of Angoumois
- L Plio-Quaternary sands of Aquitaine Basin
- M Calcareous formations of Aquitaine Basin
- N Alluvial formations of Garonne
- O Volcanic formations of Central Massif
- P Fluvio-glacial formations of Rhone valley
- Q Alluvial formations of Mediterranean region



Ratio Sen's slope/maximum WLF

(a)



(b)



■ Raw groundwater levels (monthly averages)

■ 7yrs filtered groundwater levels

■ 17yrs filtered groundwater levels

Aquifer group

■ Bedrock

■ Chalk

■ Greensands

■ Limestones

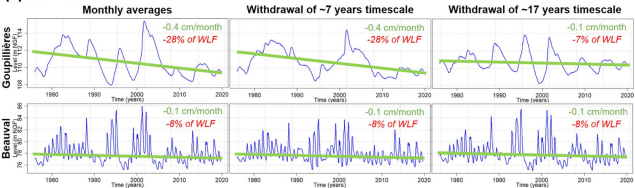
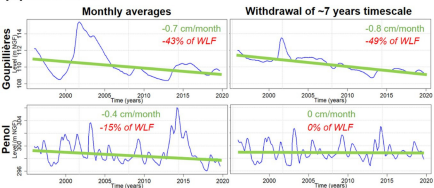
■ Not studied formations

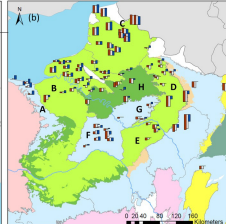
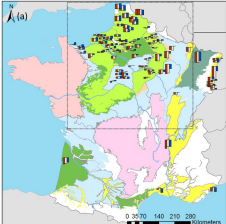
■ Sand

■ Sandstones

■ Volcanic formations

■ Alluvial formations

(a) 1976-2019**(b) 1996-2019**



Sen's slope (mm/months)

Precipitation



Raw precipitation

7-yr filtered precipitation

17-yr filtered precipitation

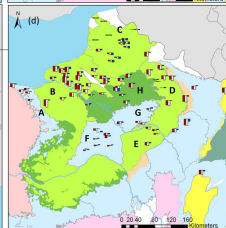
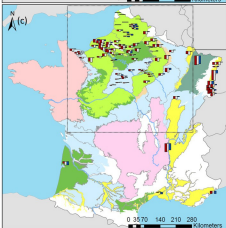
Effective precipitation



Raw effective precipitation

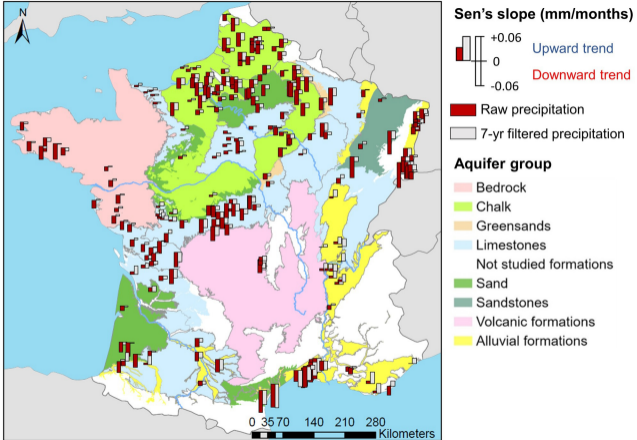
7-yr filtered effective precipitation

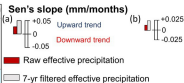
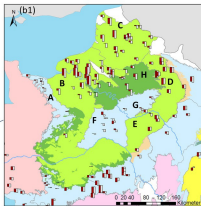
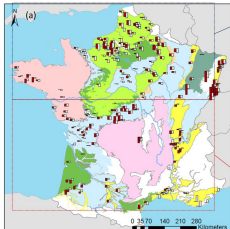
17-yr filtered effective precipitation



Aquifer group

- Bedrock
- Chalk
- Greensands
- Limestones
- Not studied formations
- Sand
- Sandstones
- Volcanic formations
- Alluvial formations





Aquifer group

- Bedrock
- Chalk
- Greensands
- Limestones
- Not studied formations
- Sand
- Sandstones
- Volcanic formations
- Alluvial formations

Hydrogeological entities

- A Jurassic limestones from Sarthe to Bessin
- B Seno-Turonian chalk of Normandy/Picardy
- C Seno-Turonian chalk of Artois-Picardy Basin
- D Chalk of Champagne
- E Upper Cretaceous chalk of Bourgogne
- F Limestones of Beauce
- G Eocene limestones of Paris Basin
- H Lutetian and Ypresian sands of Paris Basin
- I Jurassic limestones of Poitou
- J Fractured Jurassic limestones of northern Aquitaine Basin
- K Upper Cretaceous limestones of Angoumois
- L Plio-Quaternary sands of Aquitaine Basin
- M Calcareous formations of Aquitaine Basin
- N Alluvial formations of Garonne
- O Volcanic formations of Central Massif
- P Fluvio-glacial formations of Rhone valley
- Q Alluvial formations of Mediterranean region